JCI insight

LncRNA *DRAIR* is downregulated in diabetic monocytes and modulates inflammatory phenotype via epigenetic mechanisms

Marpadga A. Reddy, … , Sridevi Devaraj, Rama Natarajan

JCI Insight. 2021. https://doi.org/10.1172/jci.insight.143289.

Research In-Press Preview Inflammation Metabolism

Graphical abstract

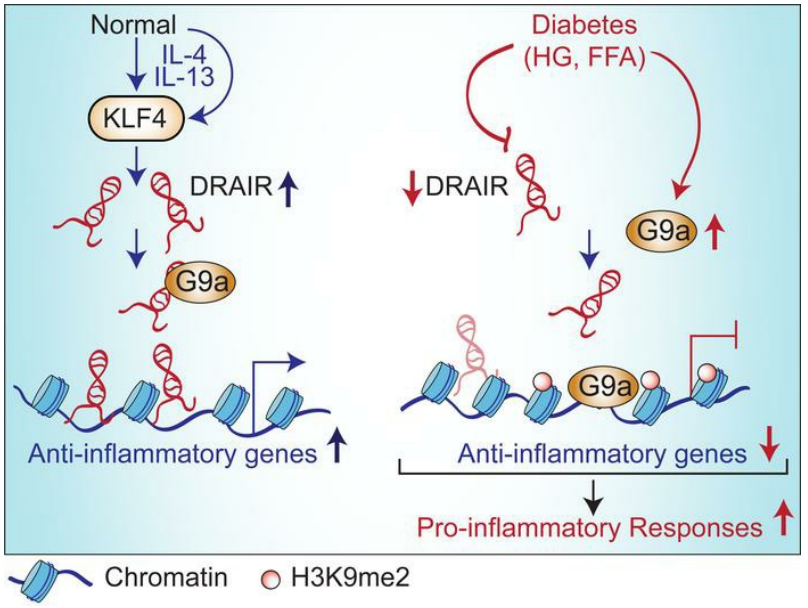

LncRNA *DRAIR* is downregulated in diabetic monocytes and modulates inflammatory phenotype via epigenetic mechanisms

Marpadga A. Reddy[1*], Vishnu Amaram [1], Sadhan Das[1,2], Vinay Singh Tanwar[1], Rituparna Ganguly[1], Mei Wang[1], Linda Lanting[1], Lingxiao Zhang[1], Maryam Abdollahi[1], Zhuo Chen[1], Xiwei Wu[3], Sridevi Devaraj[4] and Rama Natarajan[1*]

[1]Department of Diabetes Complications and Metabolism, Arthur Riggs Diabetes and Metabolism Research Institute and Beckman Research Institute of City of Hope, Duarte, CA, [2]Pharmacology Division, CSIR-Central Drug Research Institute, Lucknow, 226031, India. [3]Integrative Genomics Core, Beckman Research Institute of City of Hope, Duarte, CA, and [4]Baylor College of Medicine and Texas Children's Hospital, Houston, TX,

Short title: Inflammatory gene regulation by lncRNA *DRAIR* in monocytes

Corresponding authors:

[*]Rama Natarajan, PhD, Department of Diabetes Complications and Metabolism, Arthur Riggs Diabetes and Metabolism Research Institute and Beckman Research Institute of City of Hope, 1500 East Duarte Road, Duarte, CA 91010, Ph: 626-218-2289; Email: rnatarajan@coh.org

[*]Marpadga A Reddy, PhD, Department of Diabetes Complications and Metabolism, Arthur Riggs Diabetes and Metabolism Research Institute and Beckman Research Institute of City of Hope, 1500 East Duarte Road, Duarte, CA 91010, Ph: 626-218-3671; Email: mreddy@coh.org

Abstract

Long noncoding RNAs (lncRNAs) are increasingly implicated in the pathology of diabetic complications. Here we examined the role of lncRNAs in monocyte dysfunction and inflammation associated with human type 2 diabetes mellitus (T2D). RNA-seq analysis of $CD14^+$ monocytes from patients with T2D versus healthy controls revealed downregulation of anti-inflammatory and anti-proliferative genes along with several lncRNAs, including a novel divergent lncRNA *DRAIR* (Diabetes Regulated anti-inflammatory RNA) and its nearby gene *CPEB2*. High glucose and palmitic acid downregulated *DRAIR* in cultured $CD14^+$ monocytes, whereas anti-inflammatory cytokines and monocyte-to-macrophage differentiation upregulated *DRAIR* via KLF4 transcription factor. *DRAIR* overexpression increased anti-inflammatory and macrophage differentiation genes but inhibited pro-inflammatory genes. Conversely, *DRAIR* knockdown attenuated anti-inflammatory genes, promoted inflammatory responses, and inhibited phagocytosis. *DRAIR* regulated target gene expression through interaction with chromatin, and inhibition of the repressive epigenetic mark H3K9me2 and its corresponding methyltransferase G9a. Mouse orthologous *Drair* and *Cpeb2* were also downregulated in peritoneal macrophages from T2D db/db mice, and *Drair* knockdown in non-diabetic mice enhanced pro-inflammatory genes in macrophages. Thus, *DRAIR* modulates inflammatory phenotype of monocytes/macrophages via epigenetic mechanisms, and its downregulation in T2D may promote chronic inflammation. Augmentation of endogenous lncRNAs like *DRAIR* could serve as novel anti-inflammatory therapies for diabetic complications.

Introduction

Systemic low-grade inflammation is a hallmark of type 2 diabetes mellitus (T2D) and contributes to the pathogenesis of several associated complications, including cardiovascular disease (1, 2). Activation of monocytes and macrophages plays an important role in inflammatory processes needed for protection against invading pathogens or toxins (3). Under physiological conditions, acute inflammation self-resolves via a balancing interplay between inflammatory and anti-inflammatory mediators and is essential for tissue repair (4, 5). However, factors associated with inflammatory diseases like T2D, including high glucose (HG), elevated levels of advanced glycation end products (AGEs) and free fatty acids (e.g., palmitic acid (PA) and oxidized lipids), markedly enhance production of pro-inflammatory cytokines such as Interleukin-1 beta (IL-1β), IL-6, and tumor necrosis factor-alpha (TNF-α) and inhibit production of protective factors, leading to chronic inflammation. In addition, the diabetic milieu increases the number of monocytes (monocytosis) further increasing the burden for cardiovascular disease (5-10). Experimental studies have elucidated key molecular and signaling pathways involved in the activation of monocytes and macrophages. These include increased oxidative stress; production of reactive oxygen species; and activation of various kinases, transcription factors (TFs) (e.g., NF-κB and STAT3), inflammasomes, and toll-like receptors (5-7). Furthermore, epigenetic mechanisms have also been demonstrated in the activation of pro-inflammatory phenotype of monocytes and macrophages (11). Evidence shows that blocking inflammatory signaling using antibodies against cytokines, cytokine receptor antagonists, lipid lowering drugs, and some antioxidants could reduce risk for metabolic disease and vascular complications (12-15). However, these therapeutic strategies are not always fully effective in preventing progression and recurrence of cardio-metabolic disease. Thus, further understanding of the precise molecular mechanisms associated with chronic inflammation is needed to develop much needed new and effective therapies.

Non-coding RNAs like microRNAs (miRNAs) and long non coding RNA (lncRNA)s have emerged as key regulators of gene expression mediating functions of monocytes and macrophages such as inflammation, innate immunity, differential response to endotoxemia, cholesterol homeostasis and macrophage polarization (16, 17). LncRNAs are defined as >200 nucleotides long transcripts with no coding potential. They regulate gene transcription via diverse mechanisms depending on their subcellular localization. Nuclear lncRNAs can regulate gene expression by interacting with chromatin, or they can act as a scaffolds, decoys, or recruiters of chromatin modifying factors/complexes and TFs to alter epigenetic states at target gene promoters and enhancers. On the other hand, cytoplasmic lncRNAs can regulate functions of translation factors, signaling proteins, and miRNAs (16, 17).

Emerging evidence shows that lncRNAs can play functional roles in diabetic vascular disease (18-20). Our recent studies demonstrated the involvement of three lncRNAs in the regulation of monocyte/macrophage inflammatory phenotype in diabetes and metabolic syndrome in mice and humans. Two of these lncRNAs *E330013P06* and *Dnm3os* were upregulated in macrophages from T2D db/db mice and T2D humans relative to healthy non-diabetic controls and these lncRNAs had pro-inflammatory properties (21, 22). In contrast, another lncRNA *Mist* was downregulated in macrophages from high fat diet induced obese mice, and in adipose tissue macrophages from humans with obesity and metabolic syndrome and exhibited anti-inflammatory properties (23). Further mechanistic studies demonstrated that disruption of lncRNA-regulated epigenetic mechanisms under diabetic or obese conditions can facilitate pro-inflammatory phenotypes in macrophages (22, 23). Several lncRNAs dysregulated in cardiometabolic disease were also identified in human monocytes (24). However, very little is known about lncRNAs in human monocytes with protective effects that might assist in resolution of inflammation in T2D. Such knowledge could assist in the development of newer therapies for diabetes and its associated chronic inflammatory disorders.

In this study, we compared the transcriptome in $CD14^+$ monocytes from T2D volunteers versus monocytes from non-diabetic volunteers to gain insights into the role of differentially expressed lncRNAs in monocyte dysfunction. We found not only many inflammatory genes were upregulated, several anti-inflammatory and anti-proliferative genes were downregulated, and also several lncRNAs were dysregulated in T2D-monocytes versus controls. Among the differentially expressed lncRNAs, we selected one novel lncRNA for further characterization which we named Diabetes Regulated anti-inflammatory lncRNA (*DRAIR*). *DRAIR* expression was downregulated in T2D-monocytes and in cultured human monocytes treated with HG and PA, but upregulated by anti-inflammatory cytokines interleukin-4 (IL-4) and IL-13. Functional and mechanistic studies demonstrated that *DRAIR* increases the expression of anti-inflammatory genes via interaction with chromatin and modulation of repressive epigenetic histone modifications at target gene promoters. Furthermore, the anti-inflammatory function of *Drair* (mouse ortholog) was also observed in vivo in mice. Together, these studies demonstrate that lncRNA *DRAIR* regulates anti-inflammatory phenotype via epigenetic mechanisms in monocytes, and that its downregulation in diabetes promotes chronic inflammation.

Results

T2D is associated with reduced expression of anti-inflammatory and anti-proliferation genes in human CD14⁺ monocytes. Although evidence shows that T2D promotes monocyte activation and monocytosis associated with chronic inflammation, the dysregulated gene expression, and the regulatory role of lncRNAs in these inflammatory processes are unclear. To examine this further, we performed strand specific RNA-seq analysis to profile changes in the transcriptome of $CD14^+$ monocytes obtained from human volunteers with T2D (T2D-monocytes) relative to control healthy volunteers without diabetes (Control-monocytes) (Supplementary Table 1 and Figure 1A). T2D-monocytes exhibited extensively altered transcriptomes with upregulation of 993 genes and downregulation of 1865 genes (Fold-Change ≥ 2, Average Coverage ≥ 1, FDR ≤ 0.05, n= 5 per group) versus -control-monocytes (Figure 1B). Several inflammatory genes were upregulated (Supplementary Figure 1A) in line with previous studies (25-27). Interestingly, there was much greater reduction in the expression of several key anti-inflammatory, antioxidant and anti-proliferative genes including *IL1RN* that codes for IL-1 receptor antagonist (IL-1Ra), *SOD2 and PTEN*, in T2D-monocytes respectively (Figure 1C), suggesting T2D is associated with the loss of protective genes.

Gene Ontology (GO) analysis showed enrichment of processes associated with translation, wound healing, ncRNA processing, and immune cell activation in the upregulated genes. Downregulated genes showed enrichment of intracellular signaling, immune response, and apoptosis (Supplementary Figure 1B and C). Ingenuity Pathway Analysis (IPA) revealed enrichment of inflammatory response under the Diseases and Functions category in both the upregulated and downregulated genes (Supplementary Figure 1, D and E). Moreover, IPA also revealed enrichment of canonical pathways related to fatty acid oxidation and nitric oxide (NO) signaling among upregulated genes (Supplementary Figure 1F). Downregulated genes were enriched with several overlapping networks including NF-κB signaling, PI3K/Akt activation, nitric

oxide (NO)/reactive oxygen species (ROS) production, and the IL-6 pathway (Figure 1D and Supplementary Figure 1G). Together these data suggest that disruption of protective mechanisms/factors may activate inflammatory pathways in T2D. Motif analysis revealed that promoters of differentially expressed genes (DEGs) were enriched in binding sites for key transcription factors (TFs) such as NF-κB, Egr1, and KLF4 (Fig. 1,E and F), which are known to be involved in inflammation and macrophage polarization (28). These results suggest that T2D induced changes in the monocyte transcriptome can dysregulate genes associated with key monocyte/macrophage functions including inflammatory phenotype, apoptosis, proliferation and phagocytosis that can contribute to inflammatory diabetes complications including cardiovascular disease.

Dysregulation of lncRNAs in T2D monocytes, including a novel lncRNA DRAIR. To elucidate the role of lncRNAs in T2D-induced monocyte dysfunction, we further analyzed differentially expressed lncRNAs by assessing potential open reading frames as described (21). We found that, 335 lncRNAs were differentially expressed in T2D monocytes (Figure 2A) including those expressed from bidirectional promoters and designated as divergent transcripts (Figure 2B). Gene ontology (GO) analyses of nearby (± 250kb) DEGs revealed enrichment of inflammation and immune cell functions near downregulated lncRNAs (Supplementary Figure 2A). Whereas, metabolic processes were enriched in DEGs near upregulated lncRNAs (Supplementary Figure 2B).

Next, we tested our hypothesis that key lncRNAs downregulated in T2D may alter inflammatory phenotype of monocytes and macrophages. We focused on a differentially expressed lncRNA annotated as *CPEB2-AS* (hg19), whose regulation and function have not been previously studied. *CPEB2-AS* is divergently transcribed adjacent to the cytoplasmic element binding protein 2 (*CPEB2*) gene on human chromosome 4. Both share the same promoter as evidenced

by H3K4me3 enrichment (Figure 2C). Divergent transcripts have been reported in development (29), but their function in T2D induced inflammation is unknown. Moreover, the nearby *CPEB2* belongs to the CPEB family, which has reported anti-inflammatory functions (30), suggesting *CPEB2-AS* may regulate inflammatory pathways. Based on subsequent functional assessment studies, we renamed *CPEB2-AS* as *DRAIR* (Diabetes regulated anti-inflammatory RNA).

RNA-seq data revealed that the *DRAIR* and nearby *CPEB2* were significantly downregulated in monocytes from T2D patients (Figure 2C). Using RT-qPCR, we validated the significant downregulation of *DRAIR* and *CPEB2* in $CD14^+$ monocytes from T2D patients versus controls (Figure 2, D and E). T2D is associated with elevated blood glucose and circulating levels of free fatty acids such as PA. Therefore, we examined the effect of HG and PA in $CD14^+$ monocytes from healthy volunteers in vitro. Monocytes were cultured in normal glucose (NG, 5.5 mM,) or HG (25 mM) for 3 days. In the last 24 h, NG and HG cells were also treated with PA (200 μM), referred to as PA and HG+PA (HP) groups respectively. RT-qPCR analysis showed that, relative to NG, PA, HG or HP significantly inhibited *DRAIR* expression (Figure 2F). PA also downregulated *DRAIR* in $CD14^+$ monocytes converted to macrophages (Figure 2G). Furthermore, HG, PA and an inflammatory cytokine IL-1B (10 ng/ml, 24h), whose levels are elevated in T2D (2) also downregulated *DRAIR* expression in the human THP1 monocytic cell line (Figure 2H). These results demonstrate that lncRNA *DRAIR* is downregulated in T2D and by major pathological factors elevated in T2D, suggesting that it may regulate anti-inflammatory processes in monocytes.

Characterization of DRAIR and its subcellular localization. Bioinformatics analysis using PhyloCSF and Coding Potential Calculator 2 suggested that *DRAIR* lacks coding potential (Supplementary Fig. 3A). This was further confirmed experimentally in an in vitro coupled transcription-translation system using *DRAIR* cDNA cloned into pcDNA3.1 expression plasmid as a template which showed absence of protein products (Supplementary Figure 3B-and 3D)

similar to no template control (NTC) reactions. The positive control luciferase transcript (LUC) expressed a 62 kDa protein as expected.

Because, lncRNA functions are dependent upon subcellular localization, we next examined *DRAIR* levels in the cytoplasmic and nuclear fractions isolated from THP1 monocytes and THP1 cells differentiated into macrophages using phorbol myristate acetate (PMA, 20 ng/ml). RT-qPCR showed that *DRAIR* levels were highly enriched in nuclear fractions from THP1 monocytes and macrophages. As expected, the known nuclear lncRNA *NEAT1* and coding RNA *PPIA* showed enrichment in nuclear and cytosolic fractions, respectively (Supplementary Figure 4A to F). Nuclear localization of *DRAIR* was further confirmed by RNA-fluorescent in situ hybridization assay in THP1 macrophages using fluorescently labeled *DRAIR* probes (Supplementary Figure 4G). Furthermore, *DRAIR* was also found to be enriched in chromatin fractions versus soluble nuclear extracts similar to *NEAT1*, a known chromatin-associated lncRNA (Supplementary Figure 4, H and I) suggesting nuclear localized *DRAIR* might have functions related to transcriptional regulation in monocyte/macrophages.

DRAIR downregulates inflammatory phenotype in monocytes and macrophages. We next examined the effect of *DRAIR* on monocyte gene expression and inflammatory phenotype using both gain-of-function (overexpression) and loss-of-function (gene silencing) approaches. For overexpression experiments, we cloned *DRAIR* cDNA into a lentiviral vector. Then, transduced THP1 monocytes with lentiviruses expressing *DRAIR* (DRAIR) or a control *EGFP* (EV), and the gene expression was analyzed by RT-qPCR. Results showed that *DRAIR* overexpression (Figure 3A) upregulated the nearby *CPEB2* gene and the anti-inflammatory gene *IL1RN* (Figure 3, B and C), but downregulated pro-inflammatory genes *TNF* and *FCGR3B* (*CD16b*) (Figure 3, D and E). Furthermore, *DRAIR* overexpression also upregulated macrophage markers such as scavenger receptors *CD68* and *CD36,* and a BCL2 family member *MCL1* that regulates

apoptosis (Figure 3, F-H). These results demonstrate that lncRNA *DRAIR* may regulate macrophage functions and promote anti-inflammatory processes.

Next, we determined the effect of *DRAIR* silencing on monocyte inflammatory phenotype. THP1 cells were transfected with siRNAs targeting *DRAIR* (siDR) or negative control siRNA (siNC) and 48 h later treated with lipopolysaccharide (LPS, 100 ng/ml) for 24 h. RT-qPCR analysis showed that siDR inhibited *DRAIR* expression and nearby *CPEB2* as well as *IL1RN*, but enhanced pro-inflammatory *IL1B* expression (Figure 3, I-L). We also tested whether *DRAIR* gene silencing can downregulate *IL1RN* expression in THP1 macrophages. THP1 cells were transfected with siDR or siNC followed by treatment with PMA (20 ng/ml) to induce macrophage differentiation. PMA treatment increased *DRAIR* expression along with *IL1RN* and *CPEB2*, but *DRAIR* gene silencing by siDR significantly inhibited both *CPEB2* and *IL1RN* relative to siNC transfected cells (Figure 3, M-O), further verifying that *DRAIR* can positively regulate anti-inflammatory genes in macrophages.

We also examined whether *DRAIR* gene silencing can enhance monocyte-endothelial cell (EC) adhesion, a key indicator of inflammation. THP1 monocytes were transfected with siDR or siNC and 48 h later treated with or without TNF-α (10 ng/ml for 3h). Then, THP1 monocytes were fluorescently labeled with DAPI and incubated with primary human umbilical vein ECs plated in 24 well plates to perform adhesion assays. Monocyte-EC adhesion was significantly enhanced after *DRAIR* knockdown (Figure 3, P and Q, panels siNC versus siDR). However, TNF-α–induced increases in monocyte-EC adhesion was not further enhanced by siDR (Figure 3, P and Q, panels siNC+TNF versus siDR+TNF). These results demonstrate that *DRAIR* gene silencing promotes inflammatory phenotype in THP1 monocytes.

Phagocytosis is an important function of macrophages in normal and pathological conditions. Because, *DRAIR* is induced during macrophage differentiation, and phagocytosis related

pathways were enriched in differentially regulated genes inT2D monocytes (Supplementary Figure. 1G), we tested if *DRAIR* knockdown affects phagocytosis. We found that *DRAIR* knockdown with siDR significantly attenuated basal and IL-4 induced phagocytosis of fluorescently labeled *E. coli* bio-particles in THP1 macrophages (Figure 3R). Furthermore, LPS also inhibited phagocytosis, and this was further inhibited after *DRAIR* knockdown (Figure 3R). Together, these data clearly demonstrate that *DRAIR* regulates anti-inflammatory processes and key macrophage functions.

DRAIR knockdown amplifies and DRAIR overexpression attenuates inflammatory genes in CD14+ monocytes. Next, we examined if DRAIR can elicit similar anti-inflammatory effects in human $CD14^+$ monocytes. We differentiated $CD14^+$ monocytes isolated from non-diabetic human volunteers and transfected them with siDR or siNC. Two days post transfection, cells were treated with or without LPS and gene expression was analyzed. siDR mediated knockdown of *DRAIR* significantly enhanced LPS induced expression of *IL1B*, *TNF* and *IL6* (Fig. 4, A-D). Conversely, we examined the consequences of *DRAIR* overexpression by transfecting $CD14^+$ monocytes with *DRAIR* expression plasmid pDRAIR (DRAIR) or control empty vector pcDNA3.1 (EV). DRAIR overexpression significantly attenuated LPS induced *IL1B, TNF* and *IL6* expression (Fig. 4, E-H), clearly demonstrating that *DRAIR* mediates anti-inflammatory effects even in primary human monocytes.

DRAIR expression is induced by macrophage differentiation and by anti-inflammatory cytokines via KLF4. Monocyte to macrophage differentiation plays an important role in inflammation and homeostasis. Therefore, we examined the expression of *DRAIR* in THP1 cells that were differentiated into macrophages by treatment with PMA (20 ng/ml). We found that expressions of *DRAIR* and *CPEB2* were significantly increased in THP1 macrophages relative to monocytes at 24 h after PMA treatment (Figure 5, A and B). In parallel, anti-inflammatory *IL1RN* was upregulated and pro-inflammatory *TNF* was downregulated (Figure 5, C and D). Next, *DRAIR*

expression was examined after treatment with IL-4 and IL-13, which are known to promote alternatively activated (M2) phenotype and anti-inflammatory responses in macrophages. Both IL-4 and IL-13 (20 ng/ml, 24 h) significantly induced *DRAIR* expression (Figure 5E). In parallel, *CPEB2* and *IL1RN* were also upregulated by these two cytokines, whereas *TNF* was downregulated (Figure 5, F-H). Treatment with a mixture of IL-4 and IL-13 had no further additive effects suggesting similar pathways regulate these genes (Figure 5, E-H).

TF motif search of the *DRAIR* promoter by Transfac analysis revealed several binding sites for Kruppel-like family (KLF) members including KLF4 (Supplementary Figure 5), a reported negative regulator of macrophage inflammatory phenotype (31). Accordingly, transfection of THP1 cells with a KLF4 expression plasmid (pKLF4) significantly increased *KLF4* expression, and upregulated *DRAIR* and *CPEB2* relative to empty vector (pCD) (Figure 5, I-K). Furthermore, chromatin immunoprecipitation (ChIP) assays with KLF4 antibody confirmed KLF4 binding at the *DRAIR* promoter but not at control *PPIA* promoter (Figure 5L). To further verify whether KLF4 regulates the *DRAIR* promoter, we constructed a reporter plasmid pDRluc in which luciferase is expressed from the *DRAIR* promoter region (-1064 to +39 bp) harboring the KLF4 binding site at -760 bp (Figure 5M). Transient transfection with pDRluc showed that *DRAIR* promoter activity was inhibited by PA (200 μM) but transactivated by IL-4 (20 ng/ml) and PMA (TMac) (Figure 5, N and O). Furthermore, co-transfection of pDRluc reporter plasmid with pKLF4 plasmid induced transactivation of the *DRAIR* promoter relative to pCD, which was further enhanced after PMA treatment (Figure 5P). These results demonstrate that *DRAIR* expression is upregulated during macrophage differentiation and by anti-inflammatory cytokines and that KLF4 plays a key role in its transcriptional activation.

CPEB2 gene silencing also promotes inflammatory phenotype in THP1 monocytes. Because our data suggested that *DRAIR* could regulate the nearby gene *CPEB2* that codes for CPEB2 protein, we examined if *CPEB2* knockdown mimics the anti-inflammatory effects of DRAIR.

Transfection of THP1 cells with siRNA targeting *CPEB2* (siCPEB2) inhibited expression of both *CPEB2* and *DRAIR*, but upregulated *IL1B* and *TNF* compared with siNC transfected cells (Figure 6, A-D). Furthermore, *CPEB2* knockdown in THP1 cells also enhanced both basal and TNF-α induced monocyte-EC adhesion (Figure 6, E and F). These results suggest that CPEB2 may mediate some of the anti-inflammatory effects of *DRAIR* in THP1 cells.

ChIRP analysis reveals DRAIR binding sites on chromatin. Interactions with chromatin and chromatin-interacting proteins are major mechanisms by which nuclear lncRNAs can regulate gene expression. Because *DRAIR* is enriched in chromatin, we examined the interactions of *DRAIR* with chromatin by performing chromatin isolation by RNA purification (ChIRP) assays with THP1 nuclear lysates using biotinylated tiling oligonucleotide probes targeting the *DRAIR* RNA. RT-qPCR confirmed specific recovery of *DRAIR* transcript but not control *GAPDH* in RNA recovered from ChIRP assays (Figure 7A). DNA recovered from ChIRP assays (ChIRP-DNA) was analyzed by DNA-seq (ChIRP-seq) to identify genome wide interactions of *DRAIR*. ChIRP-seq analysis revealed 152 *DRAIR* binding sites (Dbs) on multiple chromosomes in THP1 cells (Supplementary Table 2). These Dbs were enriched at promoter, intronic, and enhancer regions on the chromatin (Figure 7B). Interestingly, 290 genes located nearby Dbs (± 250 kb, Supplementary Table 3) were differentially expressed in our RNA-seq data from T2D monocytes (Figure 1B). IPA showed that these genes nearby Dbs are involved in inflammatory response, chemotaxis and phagocytosis (Figure 7C). Transfac analysis of Dbs showed enrichment of key TFs involved in monocyte and macrophage functions, including members of the KLF family (Supplementary Figure 6).

To further understand the functions of *DRAIR* at the chromatin level, we examined the potential interaction of Dbs with other genomic regions using capture Hi-C plotter (CHiCP), a publicly available promoter capture Hi-C database in human cells (32). CHiCP analysis of human macrophages revealed interactions of Dbs with multiple genomic regions suggesting their role in

DRAIR mediated gene regulation. One of the Dbs was located in the intronic region of *OPTC* gene on chromosome 1, which we named OPTC-Dbs (Figure 7D). CHiCP analysis revealed that the OPTC-Dbs potentially interacts with a genomic region 362 kb away on the same chromosome (CHiCAGO score > 5). This Dbs interacting region is upstream of *CHIT1* and *CHI3L* genes (Figure 7E), that regulate macrophage M2 phenotype (33) .

Using candidate ChIRP-qPCR, we validated the interaction between *DRAIR* and the OPTC-Dbs in THP1 monocytes. Moreover, this interaction was abolished by RNase treatment of THP1 lysates, confirming the specificity of the interaction (Figure 7F). We next examined whether *DRAIR* regulates *CHIT1* and *CHI3L* genes. RT-QPCR analysis showed that *DRAIR* overexpression significantly upregulated *CHIT1* and *CHI3L,* but not *lnc01136*, a lncRNA expressed in the nearby region (Figure 7, G-I), suggesting that *DRAIR* may regulate these genes through interaction at OPTC-Dbs in monocytes. In addition, candidate ChIRP-qPCR also demonstrated *DRAIR* interaction with the promoter of adjacent *CPEB2* (Figure 7F), suggesting a role for chromatin interaction in the regulation of nearby *CPEB2* gene by *DRAIR*. These results indicate that *DRAIR* interactions with chromatin may play important roles in the regulation of proximally and distally located monocyte/macrophage genes.

DRAIR interacts with G9a histone methyltransferase and controls repressive histone modifications at target gene promoters. We next used ChIRP followed by mass spectrometry (ChIRP-MS) to explore whether *DRAIR* also regulates gene expression via interactions with chromatin modifying enzymes/proteins. Because endogenous *DRAIR* is not abundant in THP1 monocytes cells, we used a THP1 cell line stably overexpressing *DRAIR* for these experiments. ChIRP was performed using biotinylated tiling oligonucleotide probes complementary to DRAIR, and luciferase (*LUC*) transcript (negative control). RT-qPCR of RNA recovered from ChIRP samples (ChIRP-RNA) showed enrichment of *DRAIR* RNA only with DRAIR-probes but not with LUC-probes, confirming specificity (Figure 8A). Following ChIRP, nucleic acid-protein

complexes were fractionated by SDS-PAGE (4-15%), and the proteins captured using DRAIR or Luc probes were analyzed by mass spectrometry. ChIRP-MS analysis revealed that *DRAIR* interacts with several nuclear proteins including histone modifying enzymes, transcription repressors, and enhancer interacting proteins (Supplementary Figure 7A). STRING analysis (34) of *DRAIR* interacting proteins showed that networks of these proteins were associated with GO biological processes and molecular functions related to histone methylation, transcription, chromatin organization, and gene expression (Figure 8B and Supplementary Figure 7, B and C). These results suggest that *DRAIR* interaction with chromatin modifying protein networks may regulate epigenetic mechanisms involved in *DRAIR*-mediated gene regulation.

To examine this further, we validated *DRAIR* interaction with two proteins identified by ChIRP-MS, namely histone methyl transferases G9a (EHMT2) and SUV39H1 (KMT1A), which mediate the repressive histone modifications histone H3 lysine-9 dimethylation (H3K9me2) and H3K9me3, respectively. Previous studies showed dysregulation of H3K9me2 and H3K9me3 by hyperglycemia and diabetes in monocytes and vascular cells (11, 35). *DRAIR* interaction with G9a was validated using RNA-pulldown and RNA immunoprecipitation (RIP) assays. RNA-pulldown was performed on nuclear extracts from THP1 cells using a biotinylated *DRAIR* sense (DRAIR) probe and *DRAIR* antisense (DRAIR-AS) probe as negative control. Western blot analysis of RNA pulldown proteins revealed that G9a strongly interacts with DRAIR probe but not with DRAIR-AS probe (Figure. 8C). However, SUV39H1 protein was not detected after RNA-pulldown (data not shown). Furthermore, RIP also confirmed enrichment of *DRAIR* with G9a antibody, but not with IgG or SUV39H1 antibody (Figure 8D).

Next, we determined the effect of *DRAIR* overexpression on G9a occupancy and enrichment levels of the corresponding repressive histone modification H3K9me2 at candidate *DRAIR* target genes shown in Fig. 3, B-H. ChIP-qPCRs showed that H3K9me2 levels were significantly reduced at *IL1RN*, *CPEB2*, and *MCL1* promoters (Figure 8, E-G) in *DRAIR* overexpressing cells

(DRAIR) versus empty vector pcDNA3.1 (EV) transfected cells. These candidate genes were upregulated in *DRAIR* overexpressing cells (Figure 3). However, H3K9me2 levels were not altered at the *FCGR3B* promoter (Figure 8H). Furthermore, ChIP assays with G9a antibody showed that, in parallel, G9a occupancy was also significantly reduced at *Il1RN*, *CPEB2*, and *MCL1* promoters, but not at the *FCGR3B* promoter (Figure 8, I-L). Because H3K9me2 and G9a were not altered at the *FCGR3B* promoter and also ChIRP-MS showed interaction of *DRAIR* with EED protein, which is a part of the polycomb repressive complex-2 (PRC2) that regulates H3K27me3 repressive mark (36), we tested the impact of *DRAIR* overexpression on H3K27me3. Indeed, ChIP assays showed that *DRAIR* overexpression significantly increased H3K27me3 at the *FCGR3B* promoter (Figure 8M) whose expression was decreased under these conditions (Fig. 3E). These results suggest that *DRAIR* upregulates key target genes in part via sequestration of G9a, and downregulates other genes in part via activation of the PRC2 repressive complex in monocytes, thus implicating epigenetic mechanisms of action.

Interestingly, our RNA-seq data revealed that G9a gene (*EHMT2*) expression is upregulated in T2D monocytes versus controls (log2 fold 1.15, FDR 0.047, n=5 each). Therefore, we examined if G9a protein levels are altered in THP1 monocytes under diabetic conditions. Immunoblot analysis of nuclear extracts from THP1 monocytes treated with HG or PA alone, or HG+PA (HP) showed significant increase in G9a protein levels (Figure 8, N and O). Furthermore, *EHMT2* gene silencing with siRNA (siG9a) significantly increased expression of DRAIR target genes *IL1RN*, *CPEB2* and *MCL1* relative to non-targeting siRNA (siNTC) in THP1 cells (Supplementary Figure 8). This data suggests that downregulation of *DRAIR* and upregulation of G9a in T2D might work together, at least in part, to repress key anti-inflammatory genes.

*Mouse orthologous Drair is downregulated in macrophages from T2D mice and regulates inflammatory phenotype***.** To evaluate putative conservation across species, we next examined expression and function of mouse orthologous *Drair*. Using liftOver we found that an annotated

lncRNA *Gm7854* on mouse chromosome 5 is expressed as a divergent transcript near the mouse *Cpeb2* gene (Figure 9A) similar to the human transcript. We designated *Gm7854* as mouse *Drair* and examined its expression in peritoneal macrophages (PMs) from db/db mice, a well-known mouse model of T2D. RT-qPCR showed that *Drair* and nearby *Cpeb2* were significantly downregulated in PMs from db/db mice versus non-diabetic control db/+ mice (Figure 9, B and C), similar to human *DRAIR*. We next examined the outcome of targeting mouse *Driar* with specific locked-nucleic acid (LNA)-modified GapmeRs. Transfection of mouse RAW264.7 macrophage cell line with three GapmeRs (DRGa, DRGb, and DRGc) targeting different regions of *Drair* showed that only DRGb significantly inhibited *Drair* expression relative to control GapmeR NCG (Figure 9D). Moreover, *Drair* knockdown inhibited *Cpeb2* but upregulated *Tnf* and *Il1b* in RAW264.7 macrophages (Figure 9, E-G) compared with NCG. Interestingly, the expression of *Il1rn* was also increased (Figure 9H), possibly as a feedback response to increased inflammation.

Next, we examined the effect of *Drair* knockdown in vivo on macrophage inflammatory phenotype. Because, *Drair* is already downregulated in diabetic db/db mice macrophages, we examined whether *Drair* knockdown in non-diabetic C57BL/6 mice can elicit a diabetic-like inflammatory phenotype in macrophages. C57BL/6 mice were injected intraperitoneally with thioglycollate (3%) to induce inflammation and subsequently injected intraperitoneally with two doses (5 mg/kg) of in vivo grade *Drair* GapmeR DRGb or negative control GapmeR NCG (Figure 9I). Gene expression analyzed in PMs 24h after second dose showed that GapmeR DRGb significantly reduced *Drair* expression relative to GapmeR NCG injected mice (Figure 9J). Furthermore, *Drair* knockdown inhibited the expression of nearby *Cpeb2*, and in parallel increased the expression pro-inflammatory genes *Tnf*, *Il1b*, and *Il6* (Figure 9, L-N), whereas *Il1rn* expression was not altered (Figure 9O). Altogether, these data demonstrate that *Drair* has similar anti-inflammatory functions in mice and human macrophages.

Discussion

Here we show that several anti-inflammatory genes and anti-proliferative genes are downregulated in monocytes from T2D individuals relative to healthy controls, and that this downregulation may contribute to increased inflammatory phenotype and monocyte numbers. Notably, we demonstrate that levels of a key lncRNA, *DRAIR,* were significantly lower in monocytes from T2D subjects, as well as in primary human monocytes from non-diabetic volunteers treated with HG+PA. Our data show that *DRAIR* can promote anti-inflammatory phenotype in monocytes/macrophages and that *DRAIR* expression is regulated by the TF KLF4, which was previously identified as a negative regulator of macrophage inflammation (31). Notably, we found that *DRAIR* increases key target anti-inflammatory genes, such as *IL1RN* and *CPEB2*, in monocytes through novel epigenetic de-repression mechanisms. In addition, we found that mouse ortholog *Drair* is downregulated in macrophages of T2D mice and that its knock-down in vivo in non-diabetic mice increases expression of inflammatory genes in macrophages. These data suggest that downregulation of lncRNAs, such as *DRAIR*, that control endogenous anti-inflammatory networks, may contribute to key mechanisms leading to chronic inflammatory phenotype of monocytes in T2D and its complications.

Interestingly, IPA of downregulated genes in T2D (identified from RNA-seq) showed enrichment of NF-κB and ROS pathways. Because many of the downregulated genes, including *IL1RN*, *NFKBIA* and *TNFAIP3* (A20) and *NFE2L2* (NRF2) are well known mediators of anti-inflammatory and anti-oxidative stress mechanisms (Fig. 1C), their downregulation can augment inflammatory phenotypes. In addition, downregulation of tumor suppressors such as *PTEN* can lead to monocytosis, thus further increasing number of inflammatory monocytes. Evidence shows that monocytosis and enhanced infiltration of inflammatory monocytes in diabetes is linked with increased atherosclerosis burden (6). Together, these data show that

downregulation of key anti-inflammatory and tumor suppressor/anti-proliferative genes in T2D might lead to increased inflammatory and proliferative state of monocytes implicated in diabetes vascular complications.

The key anti-inflammatory gene, *IL1RN*, was one of the most highly downregulated genes in T2D monocytes. Its protein product IL-1Ra is a member of the IL-1 family that binds to IL-1 receptors and inhibits their responses. IL-1Ra expression is increased by pro-inflammatory agents and in chronic inflammatory diseases and plays an important role in host defense against inflammation (37). Experimental evidence from animal models and clinical trials using IL-1Ra (Anakinra) have underscored its role in curbing inflammation in diabetes and atherosclerosis (38, 39). Disruption in the balance between pathological and protective factors could promote chronic inflammation (5). Our data showing *IL1RN* is downregulated in T2D-monocytes support the presence of such imbalances and highlight the importance of further understanding the mechanisms and factors that inhibit or repress endogenous anti-inflammatory networks in T2D.

Several lncRNAs are reported to regulate inflammatory phenotype in macrophages (16), but the role of monocyte lncRNAs in human T2D is poorly understood. In this study, we demonstrated that hundreds of lncRNAs were differentially expressed in $CD14^+$ monocytes from subjects with T2D versus controls, including multiple divergent transcripts whose functions in monocyte/macrophage phenotype are not known. One of our key findings is that a divergent lncRNA *DRAIR* is downregulated in T2D and regulates anti-inflammatory functions and genes, such as *IL1RN* and *CPEB2*, in monocytes and macrophages. *IL1RN* can be induced by several agents including cytokines, viral and bacterial components and is a known anti-inflammatory factor (37). *CPEB* members are regulated by inflammation and hypoxia (30, 40), but mechanisms of their regulation and action in monocytes are unclear. Our studies uncovered novel lncRNA (*DRAIR*) dependent mechanisms in the regulation of *IL1RN* and *CPEB2*. In

addition, we also demonstrated a hitherto unknown anti-inflammatory function of *CPEB2* in monocytes. Cytoplasmic localization of CPEB2 protein suggests it may act via post-transcriptional mechanisms to regulate inflammatory genes (30, 40). Interestingly, we found *CPEB2* knockdown also reduced *DRAIR* expression suggesting post-transcriptional regulation of *DRAIR* by CPEB2 protein may also contribute to its anti-inflammatory effects.

Furthermore, we found that *DRAIR* regulates key macrophage genes (*CD68* and *CD36*) and an anti-apoptotic gene *MCL1* (41) involved in macrophage differentiation, apoptosis, and phagocytosis. Because these processes play key roles in the pathophysiological functions of macrophages associated with cardiovascular disorders like atherosclerosis (3, 6), *DRAIR* downregulation in diabetes may also accelerate inflammatory cardiovascular complications. The anti-inflammatory functions of *DRAIR* are further supported by our mouse in vivo data showing that *Drair* expression is down regulated in macrophages of T2D mice and that its knockdown in non-diabetic mice enhances macrophage inflammatory phenotype. Our experimental evidence showing *DRAIR* inhibition by diabetic milieu and *DRAIR* upregulation by mediators of alternative macrophage activation, such as anti-inflammatory cytokines and TF KLF4, further support the involvement of *DRAIR* in anti-inflammatory processes in monocyte/macrophages.

We found that *DRAIR* is enriched in nuclear and chromatin fractions. Such nuclear lncRNAs can regulate target gene expression by chromatin remodeling via interactions with chromatin and chromatin modifying enzymes to (16, 18). Our ChIRP-seq data demonstrated that *DRAIR* interacts with chromatin at the promoter of nearby *CPEB2* as well as other genomic loci on multiple chromosomes. Notably, our results uncovered a key DRAIR-chromatin binding site located in the *OPTC* gene (OPTC-Dbs) that interacts with the upstream region of *CHIT1*and *CHI3L genes* and might play key role in DRAIR-induced expression of *CHIT1* and *CHI3L,* genes associated with monocyte to macrophage differentiation (33). On the other hand, our ChIRP-seq analysis did not reveal *DRAIR*-chromatin interactions upstream of other *DRAIR* target

genes validated in this study, such as *IL1RN* and *MCL1.* However, several genes located near DRAIR binding sites (± 250 kb), including *CHIT1* discussed above, were dysregulated in T2D monocytes (Supplementary Table 3). These results indicate that *DRAIR* regulates some genes via direct interaction with chromatin, and others possibly through different mechanisms such as interaction with chromatin modifying proteins.

Accordingly, we found that interaction of *DRAIR* with the H3K9me2-methyltransferase G9a can regulate key target anti-inflammatory genes. G9a can regulate gene expression via targeting transcriptionally active chromatin and interaction with lncRNAs such as *Kcnq1ot1* in cancer (42, 43). Previous studies showed dysregulation of H3K9me2 in diabetes (35), but the role of G9a has not been explored. Interestingly, our RNA-seq data showed that G9a expression is increased in T2D monocytes, and treatment of THP1 monocytes with HG and PA also increased G9a protein levels indicating a potential role for G9a in monocyte functions in T2D. We found that *DRAIR* reduces promoter enrichment of G9a and the corresponding repressive mark H3K9me2 along with upregulation of anti-inflammatory genes such as *IL1RN* and *CPEB2*. This was further supported by our observation that *EHMT2* (G9a) knockdown could increase the expression of anti-inflammatory genes that are also regulated by *DRAIR*. Therefore, *DRAIR* downregulation and G9a upregulation in T2D may act co-operatively in mechanisms associated with downregulation of anti-inflammatory pathways in monocytes and chronic inflammation (Figure 10). However, *DRAIR* may also operate via G9a independent mechanisms, such as regulation of H3K27me3, as in the case of *FCGR3B,* but further studies are needed to examine the role of H3K27me3 in *DRAIR* functions.

Our study also has limitations. The T2D subjects evaluated were relatively young, and hence it is unclear if *DRAIR* is also dysregulated in more longstanding T2D. In addition, we could not determine whether overexpression/reconstitution of *Drair* in db/db mice or other mouse models of T2D can attenuate inflammation or metabolic parameters because the technology to

overexpress nuclear lncRNAs in vivo is not well developed. In addition, *Drair* knockdown did not inhibit *Il1rn* expression in mice PMs, instead showing a slight but not significant increase. These results suggest either a feedback response to increase inflammation or species-specific regulation. However, most importantly, *DRAIR* knockdown promoted inflammatory phenotype in both mice and humans supporting its conserved anti-inflammatory functions. But further work is needed to determine if the mouse and human orthologs operate through similar molecular mechanisms. We are also aware that genetic variations affecting the expression and function of lncRNAs can be associated with cardiometabolic disease (44, 45). Therefore, we searched *DRAIR* locus for genetic variants using The Cardiovascular Disease Knowledge Portal (https://cvd.hugeamp.org). However, we did not find any single nucleotide polymorphisms in the *DRAIR* locus that have significant association with human cardiovascular disease.

In summary, our results derived from multiple complementary approaches demonstrate that *DRAIR* regulates target gene expression in monocytes/macrophages via molecular and epigenetic mechanisms including direct interaction with chromatin and binding to key chromatin modifying proteins (Figure 10). Our findings emphasize the emerging role of anti-inflammatory lncRNAs in metabolic diseases acting via RNA binding proteins and epigenetic mechanisms (23). Further understanding of such endogenous protective factors could aid in the development of much needed therapies to ameliorate chronic inflammation and T2D complications.

Methods

Human CD14⁺ Monocytes and THP1 monocytic cell line. Fasting blood (15 ml) was collected from T2D and control volunteers (Supplementary Table 1). PBMCs from these samples were isolated and $CD14^+$ monocytes purified by negative selection using magnetic beads (Miltenyi Biotech) as described (21). RNA from these samples were used for RNA-seq analysis and RT-qPCR validation at City of Hope. For some in vitro experiments, human $CD14^+$ monocytes from healthy volunteers were obtained from All Cells, Berkeley CA. Blood samples collected at City of

Hope were used for all transfection experiments with human monocytes. The $CD14^+$ monocytes from Ficoll purified PBMC were isolated by immunomagnetic negative selection using EasySep Human Monocyte Isolation Kit (Catalog #19059, Stemcell Technologies). Human THP1 monocytic cell line (American Type Culture Collection, VA [ATCC]) was used to characterize *DRAIR* functions and mechanisms of actions. THP1 cells were cultured in RPMI containing 10% FBS, Penicillin/Streptomycin (Pen/Strp), 2 mM glutamine, 5.5 mM glucose and 50 μM β-mercaptoethanol. $CD14^+$ monocytes were cultured in same medium without β-mercaptoethanol. Where indicated, monocytes were treated with normal glucose (NG, 5.5 mM), high glucose (HG, 25 mM glucose) for 72 h, palmitic acid (PA, 200 μM) for 24 h, and HG + PA (PA added 48 h after culturing in HG). Cells were then lysed in QIAzol (Qiagen) for RNA extraction. Human primary monocytes were also differentiated into macrophages using M-CSF1 (25 ng/ml) for up to one week, while THP1 cells were differentiated using PMA (20 ng/ml, up to 48 h) and treated as indicated.

Isolation of mice peritoneal macrophage(PM)s. Male db/db mice model of T2D (BKS.Cg-$m^{+/+}lepr^{db}$/J, Cat# 00642), non-diabetic control db/+ mice, and C57BL/6 mice were obtained from Jackson Laboratories (Bar Harbor, Maine). Thioglycolate elicited PMs were isolated from 10-12 week old db/db and db/+ mice and C57BL/6 mice as described (21, 22). PMs were plated in RPMI supplemented with 11 mM glucose and Pen/Strp for 1 h, washed 3x with PBS and RNA extracted. Mouse macrophage cell line RAW264.7 (ATCC, TIB-71) was cultured as described (21) .

RNA extraction and gene expression analysis. RNA isolation and cDNA preparation were performed using RNeasy mini kit and on-column DNase I digestion (Qiagen). Real time quantitative PCRs (RT-qPCRs) were performed with indicated gene primers (Supplementary

Table 4) and using Prime Script RT Master Mix (Takarabio) or QuantiTect Reverse Transcription Kit (Qiagen) and SYBR Green reagent respectively on a 7500 Fast Real-Time PCR system (Thermo Fisher). Data were analyzed using the $2^{-\Delta\Delta Ct}$ method to determine relative gene expression after normalization with internal control genes (*RPLPO, HPRT1* and *PPIA* for human) and (*Rplp0* and *Ppia for* mouse genes) (21, 22).

RNA-seq analysis. Total RNA from $CD14^+$ monocytes of T2D and control subjects (n=5 each) was subjected to strand-specific RNA-seq on the Hi-Seq 2500 platform (Illumina). The data were analyzed using publicly available bioinformatics tools as described (21, 22). Raw sequences were aligned to the human reference genome hg19 using TopHat. RefSeq gene counts were normalized by trimmed mean of M value (TMM) method. Differentially expressed genes (DEGs) were identified using Bioconductor package edgeR using criteria of fold change ≥2, FDR<0.05, and average coverage ≥1 in at least one sample. DEGs were further analyzed by DAVID Functional Annotation Tool, IPA (Qiagen) and TRAP to identify gene ontologies, significantly enriched pathways, and enrichment of TF binding sites in the promoters respectively. The lncRNAs lacking coding potential were identified as described earlier (21, 22). Enrichment of biological processes in nearby DEGs were analyzed using Enrichr web server (46). RNA-Seq data are available through the NCBI's Gene Expression Omnibus database (GSE156122).

In vitro transcription/translation assay of DRAIR. *DRAIR* cDNA was cloned into pcDNA3.1 (+) and the resultant construct pDRAIR (Supplementary Fig. 3B) was linearized by digestion with XhoI and subjected to in vitro transcription-translation using the T7 TNT quick coupled transcription/translation system (Promega, Cat. No. L1170). In parallel reactions, luciferase transcript (positive control) and no template controls (negative control) were assayed. The

reaction products were analyzed by western blotting and proteins detected with Transcend colorimetric nonradioactive translation detection system (Promega) (22).

Transfection of plasmids and oligonucleotides: We used DsiRNAs (Integrated DNA Technologies) and pooled siRNAs (Dharmacon) to knockdown human *DRAIR* and *EHMT2* (G9a) respectively, and LNA-modified Gapmers (Qiagen) to target mouse *Drair*. THP1 monocytes, THP-1 differentiated into macrophages (PMA, 20 ng/ml, 24-48h), human $CD14^+$ monocytes differentiated into macrophages (M-CSF, 25-50 ng/ml for 7 days), and mouse RAW macrophages were transfected with indicated DsiRNs or siRNAs (20 nM) or Gapmers (50-100 nM) using RNAiMAX (Thermo Fisher) or TransIT-KO (Mirusbio) following manufacturers' protocols. Cells were used 48-72 h post transfection for downstream analyses.
To overexpress *DRAIR*, freshly isolated $CD14^+$ monocytes were transfected with DRAIR expression plasmid (pDRAIR) or control pcDNA3.1 (EV) using Human Monocyte Nucleofector® Kit (Lonza) on a Nucleofector device II and program Y-001. Next day, transfected cells were treated ± LPS (100 ng/ml) for 24 h and RNA isolated. THP1 cells were also transfected with pDRAIR or control pcDNA3.1 (EV) with TransIT-2020 (Mirusbio), and stably transfected cells selected using G418 (400 ug/ml). In some experiments *DRAIR* cDNA was cloned into lentiviral vector pLentipuro (AddGene). Lentiviruses expressing *DRAIR* or control *EGFP* were prepared using co-transfection with helper plasmids in HEK293T cells. THP1 cells were transduced with *DRAIR* and *EGFP* lentiviruses using polybrene (Sigma, 8 ug/ml) overnight and used a week after transduction.

Mouse *Drair* knockdown in vivo: Male C57BL/6 mice (8 weeks old) were injected (intraperitoneal) with thioglycolate (3%) followed by intraperitoneal injection of in vivo grade

Drair Gapmer or negative control Gapmer (Qiagen) at 24 and 72 h (5 mg/kg). PMs were isolated at 96 h for gene expression analysis.

Cloning of DRAIR promoter and transfection of reporter plasmids: Human *DRAIR* promoter (-1064 to +39) was PCR amplified from genomic DNA and subcloned upstream of firefly luciferase gene to generate pDRluc. THP1 cells were co-transfected with pDRluc, internal control SV40-Renilla luciferase and indicated plasmids using TransIT-2020. Following day, treatments were as indicated for 24 h, and luciferase activities in cell lysates determined using Dual-Luciferase® Reporter Assay System in GloMax Luminometer (Promega). Firefly/Renilla ratios were reported as fold over controls.

Phagocytosis assays. THP1 cells differentiated into macrophages were transfected with siDR or negative control siRNAs and treated as indicated. Next day, phagocytosis assays were performed in 96 well black plates with clear flat bottom using FITC-labeled *E. coli* BioParticles as described by the manufacturer (Vybrant Phagocytosis Assay Kit, Thermo Fisher Scientific). Fluorescence from phagocytosed *E.coli* bioparticles was measured at 483/518 nm on an Infinite 200Pro plate reader (Tecan) and results reported as arbitrary fluorescence units.

*RNA isolation from nuclear, cytoplasmic, and chromatin fractions***:** RNA from nuclear and cytosolic fractions was purified using columns and protocols supplied with PARIS kit (Thermo Fisher Scientific). RNA fractions from chromatin and soluble nuclear extracts were isolated as described (22, 23). Levels of indicated transcripts levels were determined by RT-qPCR.

*RNA-FISH***:** RNA-FISH was performed with LNA-Cy5 labeled oligonucleotide probes targeting *DRAIR* (EXIQON-QIAGEN) as described (22). Images were captured and processed using a Zeiss Observer Z1 wide field microscope and ZEN Blue software (Zeiss).

Western blot analysis: THP1 cells were treated as indicated with NG, HG, PA, and HG+PA (HP) and centrifuged at 100 g for 10 min at 4^0C. Cell pellets were washed with cold PBS and lysed in Nuclear Isolation Buffer (NEB) containing 0.25 M sucrose, 8 mM Tris HCl (pH7.4), 5 mM $MgCl_2$, 0.8% Triton X-100 and 1x Complete Protease inhibitor (Roche) on a rotator for 20 min at 4°C. Cell lysates were centrifuged at 2500 g for 20 min at 4°C, nuclear pellets lysed in Laemmli sample buffer (without dye and β-mercaptoethanol) and briefly sonicated (15 sec at 4°C, Diagenode) to reduce viscosity. Protein concentrations were estimated using Protein Assay kit (BioRad) and equal amounts of nuclear proteins were subjected to western blotting with G9a antibody (1:1000, Cat# 688851S, Cell Signaling) and internal control Histone H3 antibody (1:3000, Cat# ab1791, Abcam) (22). Intensities of protein bands detected by enhanced chemiluminescence were quantified using a GS-900 calibrated densitometer and Image Lab software (Bio-Rad). Results were expressed as the ratio of G9a/H3.

ChIRP: *DRAIR* interaction with chromatin and with nuclear proteins were determined using ChIRP assays and ChIRP followed by Mass spectrometry (ChIRP-MS) respectively (47, 48). For ChIRP assays,THP1 cells (80 million) were fixed with glutaraldehyde for 30 min, washed and lysed in ChIRP lysis buffer containing SUPERase-in RNA inhibitor (Thermo Fisher) and Complete protease inhibitors (Roche). Lysates were sonicated in Bioruptor to fragment DNA (200-1000 bp) and diluted with hybridization buffer (1:2). Then DRAIR tiling biotinylated oligonucleotides (Stellaris) were added (10 pg/ml) and incubated overnight at 37°C. The following day, ChIRP complexes were captured using streptavidin-magnetic beads and washed 5 times, and ChIRP-RNA and ChIRP-DNA eluted from the beads. ChIRP-RNA was used to estimate *DRAIR* recovery. ChIRP-DNA was used for DNA-seq on Illumina platform (HiSeq 2500). RAW reads were aligned to the human hg19 reference genome, and *DRAIR* binding sites (Dbs) on chromatin identified as described (47). ChIRP-Seq data are available through the

NCBI's Gene Expression Omnibus database (GSE156122). ChIRP-DNA was also analyzed by qPCR to validate Dbs with specific primers.

To identify *DRAIR* interacting proteins, THP1 cells stably overexpressing *DRAIR* (400 million) were fixed with formaldehyde (3%) for 30 min (48), and cell lysates were processed as described for ChIRP. Biotinylated oligonucleotides targeting luciferase (LUC) transcript were used as negative control. Nucleic acid-protein complexes were captured using streptavidin-magnetic beads, boiled in SDS-Laemmli protein sample buffer, and eluted proteins fractionated on precast SDS-PAGE (4-15%) gels (BioRad). Gels were stained with SimplyBlue SafeStain and different regions from each lane (*DRAIR* and *LUC* probes) were subjected to MASS spectrometry at City of Hope's Mass Spectrometry Core as described (22, 23). Differentially interacting proteins with *DRAIR* versus LUC probes were analyzed using Scaffold 3.0. *DRAIR* interacting proteins were further analyzed by STRING database to identify enrichment of biological processes (34) and validated using RNA pulldown and RIP assays.

RNA Immunoprecipitation (RIP) assays: THP1 cells were fixed with formaldehyde (1%) for 10 min at room temperature, washed with ice cold PBS, lysed in nuclear isolation buffer supplemented with RNase and protease inhibitors, and centrifuged at 2500 g for 20 min at 4°C to collect the nuclear pellet. Nuclei were lysed in RIPA buffer, sonicated, and immunoprecipitated overnight at 4°C with G9a antibody (5 µg, Cat # 68851S), SUV39H1 antibody (5 µg, Cat# 8729S), or negative control IgG (Cat# 2729S)(all from Cell Signaling). Immune complexes were collected on IgG-magnetic beads, washed five times with RIPA buffer, and incubated in elution buffer containing proteinase K at 55°C for 30 min. RNA from supernatants was purified using RNeasy MinElute Cleanup Kit (Qiagen) and analyzed by RT-qPCR.

RNA pull-down assays: The pcDNA3.1 (+) plasmid expressing DRAIR (pDRAIR) and pcDNA3.1(-) expressing DRAIR-anti-sense (pDRAIR-AS, Supplementary Fig. 3C) were linearized to prepare biotinylated DRAIR and DRAIR-AS probes respectively by in vitro transcription with T7-RNA polymerase using Biotin RNA Labeling Mix kit (Roche). Nuclear extracts from THP1 cells (1 mg protein) were incubated with 1 µg of biotinylated probes, and RNA pulldown assays performed as described (22). Proteins eluted from biotinylated RNA-Protein complexes were subjected to immunoblotting with G9a antibody (1:1000). Protein bands were detected using Enhanced Chemiluminescence kit (Perkin Elmer).

Chromatin immunoprecipitation (ChIP): ChIP assays were performed as described previously (22, 49) with some modifications. THP1 cells crosslinked with 1% formaldehyde were lysed in nuclear isolation buffer (20 min, 4°C) and centrifuged (2500 g, 20 min) at 4°C. Nuclear pellets were lysed in ChIP lysis buffer, and chromatin was sheared by sonication using a Bioruptor. Sonicated nuclear lysates were diluted 1:10 and lysates containing equal amounts of DNA were immunoprecipitated using antibodies against H3K9me2 (Cat# 4658S), G9a (Cat # 68851S) or H3K27me3 (Cat # 9733S) obtained from Cell Signaling, or KLF4 (10 µg, Cat# AF3640, R&D Systems). Immune-complexes were captured using IgG-magnetic beads, washed and eluted as indicated (22, 49) except that high salt wash was performed two times. ChIP DNA was reverse crosslinked overnight at 67°C and treated with RNAse A (10 µg/ml) for 30 min at 37 °C. DNA was extracted using QIAquick PCR Purification Kit. ChIP-DNA was analyzed in triplicate by qPCR using indicated primers and SYBR Green reagent on the 7500 Fast Real-Time PCR system. The qPCR data was analyzed using the formula $2^{\wedge\text{-(CtChIP-Ct100\%input)}}$ and results normalized with input were expressed as % of Input.

THP1 monocyte-endothelial cell binding assays: THP1 monocytes transfected with siDR or siNC were treated ± TNF-α for 5 h (10 ng/ml) and labeled with DAPI (5 ng/ml, 20 min), washed

twice with PBS. Then, labeled monocytes (125,000 per cm^2) were incubated with confluent Human Umbilical Vein Endothelial Cells (ECs) in 24-well plates in serum depletion medium (MCDB-131 from Sigma containing 2.5% FBS and 1x antibiotic/antimycotic agents) for 30 min at 37°C. Non-adherent monocytes were removed by washing twice with PBS. EC-bound monocytes were fixed with 1% paraformaldehyde for 15 min, washed and images from multiple wells/group captured using a fluorescence microscope (10x magnification). Bound monocytes were counted with Image J software, and results expressed as monocytes/field (Mean±SD).

*Statistical analysis***.** Graphpad Prism (7.0 and above) software was used to perform statistical analysis. Data are represented as Mean±SD of experiments performed at least in triplicate. Shapiro-Wilk normality test was used to test normal distribution of each sample group. Comparisons between two groups were performed using 2-tailed unpaired t-tests. Comparison amongst more than 2 groups were performed using ANOVA followed by multiple comparison tests as indicated in the figure legends. P-values <0.05 were considered statistically significant**.**

Study approval: All human blood samples were collected after written informed consent from T2D and Control volunteers. The study was approved by the Institutional Review Boards at City of Hope and Baylor College of Medicine. Mouse studies were approved by Institutional Animal Care and Use Committee at City of Hope and conducted in accordance with the NIH guidelines for the care and use of laboratory animals.

Author contributions

M. A. R. conceptualized the work, designed and performed most experiments, and wrote the manuscript. V. A., R. G., M. W., L. L., L. Z. and M. A. performed experiments and analyzed data. X. W. Z. C. and V. T. performed bioinformatics analysis. S.D. (City of Hope) performed experiments, assisted with experimental design, and edited the manuscript. S. D. (Baylor College) provided human monocytes for RNA-seq analysis. R. N. conceptualized the work, edited the manuscript, acquired funding, and supervised the study. R. N. and M. A. R. are the guarantors of this work and, as such, had full access to all the data in the study and take responsibility for the integrity of the data and the accuracy of the data analysis.

Acknowledgements

We are grateful to the Integrative Genomics Core (City of hope) for assistance with analysis of RNA-seq and ChIRP-seq data, and the Proteomics Core (City of Hope) for mass spectroscopy analysis of ChIRP samples. We thank Dr. Harry Scott and Dr. Kaustabh Ghosh (University of California Riverside, CA) for assistance with endothelial cell and monocyte binding studies. Research reported in this publication included work performed in the Integrative Genomics, DNA/RNA Synthesis, and Mass Spectrometry and Proteomics Cores (supported by the National Cancer Institute of the National Institutes of Health (NIH) under grant number P30CA033572), and the Light Microscopy Core of City of Hope. The content is solely the responsibility of the authors and does not necessarily represent the official views of the National Institutes of Health.

Sources of Funding. This study was supported by grants from the NIH: R01 DK065073, R01 HL106089, and R01 DK081705 (to RN) and a pilot grant from the Arthur Riggs Diabetes and Metabolism Research Institute of City of Hope (to MAR). VA was supported by a Predoctoral fellowship grant and RG by a Postdoctoral fellowship grant, both from the American Heart Association.

Conflict of interest. The authors declare no competing interests.

References

1. Bhupathiraju SN, and Hu FB. Epidemiology of Obesity and Diabetes and Their Cardiovascular Complications. *Circ Res.* 2016;118(11):1723-35.
2. Donath MY. Targeting inflammation in the treatment of type 2 diabetes: time to start. *Nat Rev Drug Discov.* 2014;13(6):465-76.
3. Murray PJ, and Wynn TA. Protective and pathogenic functions of macrophage subsets. *Nat Rev Immunol.* 2011;11(11):723-37.
4. Serhan CN, and Levy BD. Resolvins in inflammation: emergence of the pro-resolving superfamily of mediators. *J Clin Invest.* 2018;128(7):2657-69.
5. Rask-Madsen C, and King GL. Vascular complications of diabetes: mechanisms of injury and protective factors. *Cell Metab.* 2013;17(1):20-33.
6. Kanter JE, Hsu CC, and Bornfeldt KE. Monocytes and Macrophages as Protagonists in Vascular Complications of Diabetes. *Front Cardiovasc Med.* 2020;7:10.
7. Forbes JM, and Cooper ME. Mechanisms of diabetic complications. *Physiol Rev.* 2013;93(1):137-88.
8. Nagareddy PR, Murphy AJ, Stirzaker RA, Hu Y, Yu S, Miller RG, et al. Hyperglycemia promotes myelopoiesis and impairs the resolution of atherosclerosis. *Cell Metab.* 2013;17(5):695-708.
9. Lamharzi N, Renard CB, Kramer F, Pennathur S, Heinecke JW, Chait A, et al. Hyperlipidemia in concert with hyperglycemia stimulates the proliferation of macrophages in atherosclerotic lesions: potential role of glucose-oxidized LDL. *Diabetes.* 2004;53(12):3217-25.
10. Esposito K, Nappo F, Marfella R, Giugliano G, Giugliano F, Ciotola M, et al. Inflammatory cytokine concentrations are acutely increased by hyperglycemia in humans: role of oxidative stress. *Circulation.* 2002;106(16):2067-72.
11. Reddy MA, Zhang E, and Natarajan R. Epigenetic mechanisms in diabetic complications and metabolic memory. *Diabetologia.* 2015;58(3):443-55.
12. Malozowski S, and Sahlroot JT. Interleukin-1-receptor antagonist in type 2 diabetes mellitus. *N Engl J Med.* 2007;357(3):302-3.
13. Donath MY. Multiple benefits of targeting inflammation in the treatment of type 2 diabetes. *Diabetologia.* 2016;59(4):679-82.
14. Back M, and Hansson GK. Anti-inflammatory therapies for atherosclerosis. *Nat Rev Cardiol.* 2015;12(4):199-211.
15. Ridker PM, Danielson E, Fonseca FA, Genest J, Gotto AM, Jr., Kastelein JJ, et al. Reduction in C-reactive protein and LDL cholesterol and cardiovascular event rates after initiation of rosuvastatin: a prospective study of the JUPITER trial. *Lancet.* 2009;373(9670):1175-82.
16. Chen YG, Satpathy AT, and Chang HY. Gene regulation in the immune system by long noncoding RNAs. *Nat Immunol.* 2017;18(9):962-72.
17. Fitzgerald KA, and Caffrey DR. Long noncoding RNAs in innate and adaptive immunity. *Curr Opin Immunol.* 2014;26:140-6.
18. Leung A, Amaram V, and Natarajan R. Linking diabetic vascular complications with LncRNAs. *Vascul Pharmacol.* 2019;114:139-44.
19. Simion V, Haemmig S, and Feinberg MW. LncRNAs in vascular biology and disease. *Vascular pharmacology.* 2019;114:145-56.
20. Das S, Reddy MA, and Natarajan R. Role of epigenetic mechanisms regulated by enhancers and long noncoding RNAs in cardiovascular disease. *Curr Opin Cardiol.* 2020;35(3):234-41.

21. Reddy MA, Chen Z, Park JT, Wang M, Lanting L, Zhang Q, et al. Regulation of inflammatory phenotype in macrophages by a diabetes-induced long noncoding RNA. *Diabetes.* 2014;63(12):4249-61.
22. Das S, Reddy MA, Senapati P, Stapleton K, Lanting L, Wang M, et al. Diabetes Mellitus-Induced Long Noncoding RNA Dnm3os Regulates Macrophage Functions and Inflammation via Nuclear Mechanisms. *Arterioscler Thromb Vasc Biol.* 2018;38(8):1806-20.
23. Stapleton K, Das S, Reddy MA, Leung A, Amaram V, Lanting L, et al. Novel Long Noncoding RNA, Macrophage Inflammation-Suppressing Transcript (MIST), Regulates Macrophage Activation During Obesity. *Arterioscler Thromb Vasc Biol.* 2020;40(4):914-28.
24. Zhang H, Xue C, Wang Y, Shi J, Zhang X, Li W, et al. Deep RNA Sequencing Uncovers a Repertoire of Human Macrophage Long Intergenic Noncoding RNAs Modulated by Macrophage Activation and Associated With Cardiometabolic Diseases. *J Am Heart Assoc.* 2017;6(11):e007431.
25. Devaraj S, Dasu MR, and Jialal I. Diabetes is a proinflammatory state: a translational perspective. *Expert Rev Endocrinol Metab.* 2010;5(1):19-28.
26. Shanmugam N, Reddy MA, Guha M, and Natarajan R. High glucose-induced expression of proinflammatory cytokine and chemokine genes in monocytic cells. *Diabetes.* 2003;52(5):1256-64.
27. Yun JM, Jialal I, and Devaraj S. Epigenetic regulation of high glucose-induced proinflammatory cytokine production in monocytes by curcumin. *J Nutr Biochem.* 2011;22(5):450-8.
28. Murray PJ. Macrophage Polarization. *Annu Rev Physiol.* 2017;79:541-66.
29. Luo S, Lu JY, Liu L, Yin Y, Chen C, Han X, et al. Divergent lncRNAs Regulate Gene Expression and Lineage Differentiation in Pluripotent Cells. *Cell Stem Cell.* 2016;18(5):637-52.
30. Ivshina M, Alexandrov IM, Vertii A, Doxsey S, and Richter JD. CPEB regulation of TAK1 synthesis mediates cytokine production and the inflammatory immune response. *Mol Cell Biol.* 2015;35(3):610-8.
31. Liao X, Sharma N, Kapadia F, Zhou G, Lu Y, Hong H, et al. Kruppel-like factor 4 regulates macrophage polarization. *J Clin Invest.* 2011;121(7):2736-49.
32. Schofield EC, Carver T, Achuthan P, Freire-Pritchett P, Spivakov M, Todd JA, et al. CHiCP: a web-based tool for the integrative and interactive visualization of promoter capture Hi-C datasets. *Bioinformatics.* 2016;32(16):2511-3.
33. Di Rosa M, Malaguarnera G, De Gregorio C, Drago F, and Malaguarnera L. Evaluation of CHI3L-1 and CHIT-1 expression in differentiated and polarized macrophages. *Inflammation.* 2013;36(2):482-92.
34. Szklarczyk D, Gable AL, Lyon D, Junge A, Wyder S, Huerta-Cepas J, et al. STRING v11: protein-protein association networks with increased coverage, supporting functional discovery in genome-wide experimental datasets. *Nucleic Acids Res.* 2019;47(D1):D607-D13.
35. Miao F, Wu X, Zhang L, Yuan YC, Riggs AD, and Natarajan R. Genome-wide analysis of histone lysine methylation variations caused by diabetic conditions in human monocytes. *J Biol Chem.* 2007;282(18):13854-63.
36. Chittock EC, Latwiel S, Miller TC, and Muller CW. Molecular architecture of polycomb repressive complexes. *Biochem Soc Trans.* 2017;45(1):193-205.
37. Arend WP, Malyak M, Guthridge CJ, and Gabay C. Interleukin-1 receptor antagonist: role in biology. *Annu Rev Immunol.* 1998;16:27-55.
38. Larsen CM, Faulenbach M, Vaag A, Volund A, Ehses JA, Seifert B, et al. Interleukin-1-receptor antagonist in type 2 diabetes mellitus. *N Engl J Med.* 2007;356(15):1517-26.

39. Libby P. Interleukin-1 Beta as a Target for Atherosclerosis Therapy: Biological Basis of CANTOS and Beyond. *J Am Coll Cardiol.* 2017;70(18):2278-89.
40. Chen PJ, and Huang YS. CPEB2-eEF2 interaction impedes HIF-1alpha RNA translation. *EMBO J.* 2012;31(4):959-71.
41. Daigneault M, Preston JA, Marriott HM, Whyte MK, and Dockrell DH. The identification of markers of macrophage differentiation in PMA-stimulated THP-1 cells and monocyte-derived macrophages. *PLoS One.* 2010;5(1):e8668.
42. Long Y, Wang X, Youmans DT, and Cech TR. How do lncRNAs regulate transcription? *Sci Adv.* 2017;3(9):eaao2110.
43. Cao H, Li L, Yang D, Zeng L, Yewei X, Yu B, et al. Recent progress in histone methyltransferase (G9a) inhibitors as anticancer agents. *Eur J Med Chem.* 2019;179:537-46.
44. Giral H, Landmesser U, and Kratzer A. Into the Wild: GWAS Exploration of Non-coding RNAs. *Front Cardiovasc Med.* 2018;5:181.
45. Foulkes AS, Selvaggi C, Cao T, O'Reilly ME, Cynn E, Ma P, et al. Nonconserved Long Intergenic Noncoding RNAs Associate With Complex Cardiometabolic Disease Traits. *Arterioscler Thromb Vasc Biol.* 2021;41(1):501-11.
46. Kuleshov MV, Jones MR, Rouillard AD, Fernandez NF, Duan Q, Wang Z, et al. Enrichr: a comprehensive gene set enrichment analysis web server 2016 update. *Nucleic Acids Res.* 2016;44(W1):W90-7.
47. Chu C, Qu K, Zhong FL, Artandi SE, and Chang HY. Genomic maps of long noncoding RNA occupancy reveal principles of RNA-chromatin interactions. *Mol Cell.* 2011;44(4):667-78.
48. Chu C, Zhang QC, da Rocha ST, Flynn RA, Bharadwaj M, Calabrese JM, et al. Systematic discovery of Xist RNA binding proteins. *Cell.* 2015;161(2):404-16.
49. Das S, Senapati P, Chen Z, Reddy MA, Ganguly R, Lanting L, et al. Regulation of angiotensin II actions by enhancers and super-enhancers in vascular smooth muscle cells. *Nat Commun.* 2017;8(1):1467.

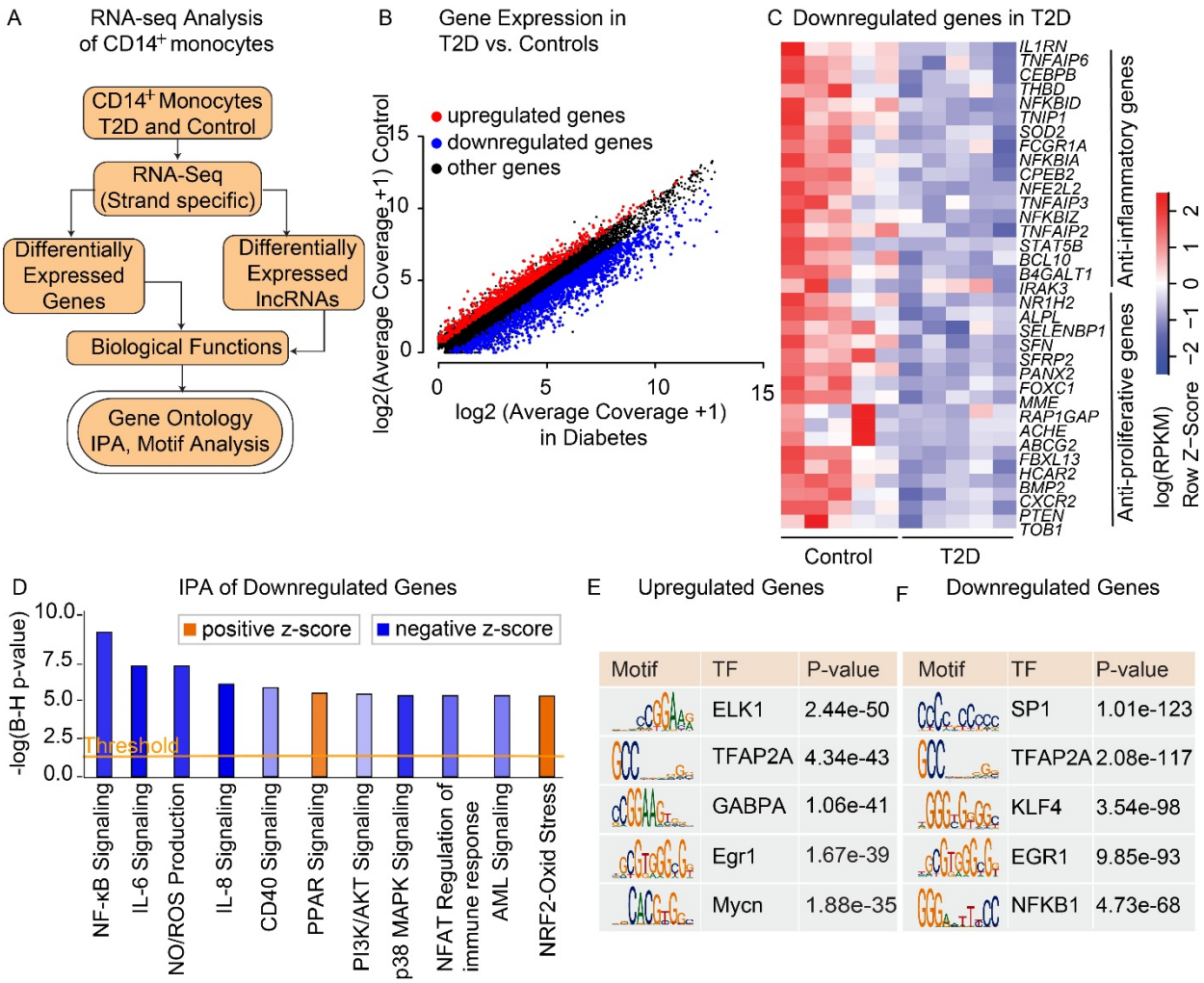

Figure 1. Type 2 Diabetes inhibits anti-inflammatory and anti-proliferation genes in human CD14⁺ monocytes.

(**A**) Scheme showing RNA-seq analysis pipeline and downstream analyses of CD14⁺ monocytes from volunteers with and without T2D. IPA-Ingenuity pathway analysis. (**B**) Scatter plot of differentially expressed genes (DEGs) in T2D monocytes versus controls (log2 fold change =>2, FDR <0.05 versus control monocytes, n=5 each). (**C**) Heatmap showing downregulation of key anti-inflammatory and anti-proliferative genes in T2D monocytes. (**D**) Enrichment of canonical signaling pathways associated with inflammation in downregulated genes. (B-H refers to: Benjamini-Hochberg). (**E-F**) Transcription factor (TF) motifs enriched in the promoters (-1000 bp

to +500 bp) of DEGs in T2D monocytes. Adjusted p-values (Benjamini-Hochberg method) are shown.

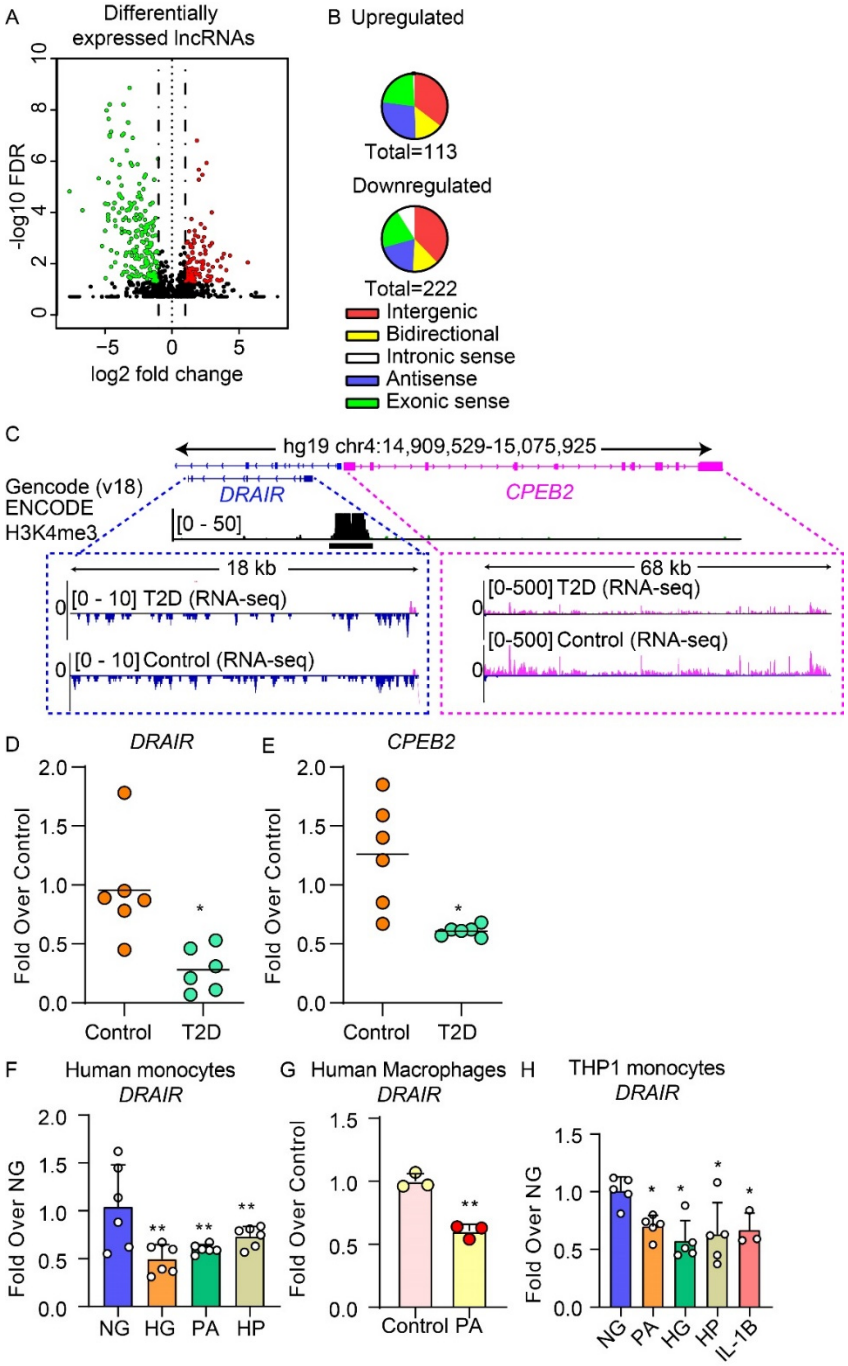

Figure 2. Dysregulation of lncRNA *DRAIR* in type 2 diabetes.

(**A-B**) Volcano plot of differentially expressed lncRNAs in T2D monocytes versus controls (**A**) and their genomic classification (**B**). (**C**) Schematic showing genomic organization of lncRNA *DRAIR* and nearby *CPEB2* gene along with RNA-seq tracks from CD14^{+} monocytes from T2D and control subjects. Both genes show downregulation in T2D. H3K4me3 track from CD14^{+}

monocytes (from ENCODE) is shown to indicate shared promoter region for both genes. Map not drawn to scale. (**D-E**) RT-qPCR validation of *DRAIR* and *CPEB2* downregulation in T2D monocytes versus control (*, P<0.05, by *t*-tests, n=6). (**F-H**) RT-qPCR results showing downregulation of *DRAIR* in primary human $CD14^+$ monocytes (F), primary human macrophages (G), and THP1 monocytes (H) treated with normal glucose (NG, 5.5 mM), high glucose (HG, 25 mM, 72 h), palmitic acid (PA, 200 μM, 24 h), and HG+PA (HP) and IL-1β (10 ng/ml). *, p<0.05 and **, p<0.01, as determined by ANOVA and Dunnett's multiple comparisons test in panels F and H, (n=3-6) and *t*-test in panel G (n=3).

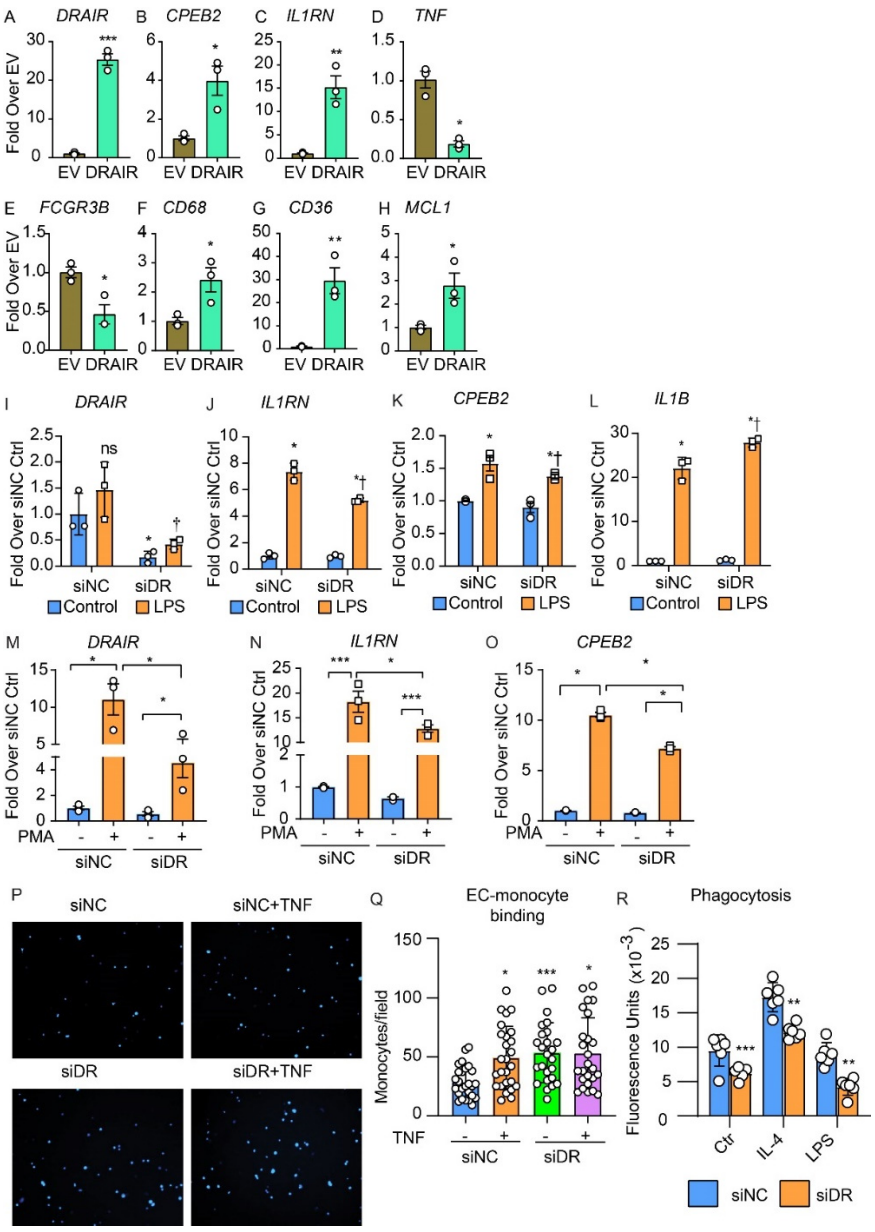

Figure 3. Effect of *DRAIR* overexpression or knockdown on pro-inflammatory gene expression and phenotype of THP1 monocytes.

(**A-H**) Effects of *DRAIR* overexpression. RT-qPCR analysis of indicated genes in THP1 cells transduced with lentivruses expressing *DRAIR* (DRAIR) or a control vector (EV).

*, p<0.05; **, p<0.01; ***, p<0.001, by t-test (n=3). (**I-L**) Effects of *DRAIR* kockdown with siRNAs. THP1 cells were transfected with control siRNA (siNC) or siRNA targeting *DRAIR*

(siDR). Two days later, cells were treated with or without with LPS (100 ng/ml) for 24 h, and gene expresion analyzed by RT-qPCR. Results expressed as fold over siNC Control. (**M-O**) RT-qPCR analysis of THP1 cells transfected with siNC or siDR treated ± PMA (20 ng/ml) for 24 h. Results expressed as fold over siNC Control (Ctrl). For **I-O**, *, $p<0.05$; **, $p<0.01$; ***, $p<0.001$ vs siNC Control and †, $p<0.05$ vs siNC LPS as determined by ANOVA and Sidak's multiple comparisons test (n=3). (**P-Q**) THP1 cells transfected with siDR or siNC were treated ± TNF-α (10 ng/ml, 3 h), labeled with DAPI and used in monocyte-endothelial cell (EC) adhesion assays. Images of bound monocytes were collected using a fluorescent microscope (**P**). Bound monocytes from multiple wells/group were quantified using Image J software (**Q**). *, $p<0.05$; ***, $p<0.001$ as determined by ANOVA and Sidak's multiple comparisons test (versus siNC Control, n=25-29). (**R**) Phagocytosis assays were performed with fluorescently labeled *E. coli* bioparticles in THP1 macrophages transfected with siDR or siNC and treated with IL-4 (20 ng/ml) or LPS (100 ng/ml) for 24h. Results shown as fluorescence from phagocytosed particles. ***, $p<0.001$ and **, $p<0.01$ as determined by Dunn's multiple comparisons test (versus siNC, n=6).

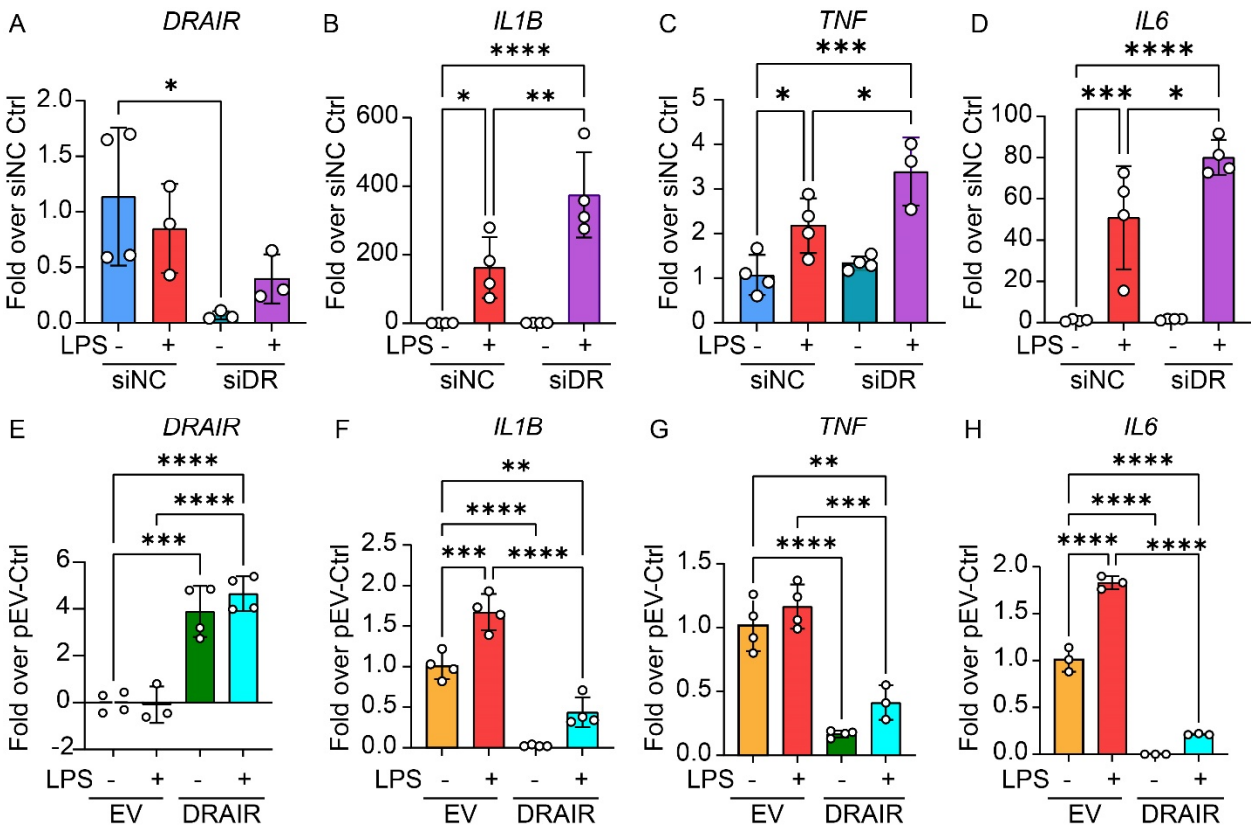

Figure 4. *DRAIR* regulates inflammatory phenotype of primary human CD14⁺monocytes. (A-D) DRAIR kockdown enhances inflammatory gene expression in human CD14+ monocytes. RT-qPCR analysis of indicated genes in CD14+ monocytes transfected with siDR or siNC. Two days after transfection, cells were treated with or without LPS (100 ng/ml) for 24 h and gene expresion analyzed by RT-qPCR. Results expressed as fold over siNC Control (Ctrl). *, p<0.05; **, p<0.01; ***, p<0.001; ****, p<0.0001 versus siNC-LPS, as determined by ANOVA followed by multiple comparison tests (n=4). Similar results were obtained with CD14+ monocytes isolated from two other volunteers. (E-H) DRAIR overexpression inhibits inflammatory phenotype in primary human CD14+ monocytes. CD14+ monocytes transfected with DRAIR expression plasmid pDRAIR (DRAIR) or empty vector pcDNA3.1 (EV) were treated with LPS (100 ng/ml) for 24 h and

expression of indicated genes analyzed by RT-qPCR (n=4). **, $p<0.01$; ***, $p<0.001$; ****, $p<0.0001$ as determined by one way ANOVA and multiple comparison tests (n=4).

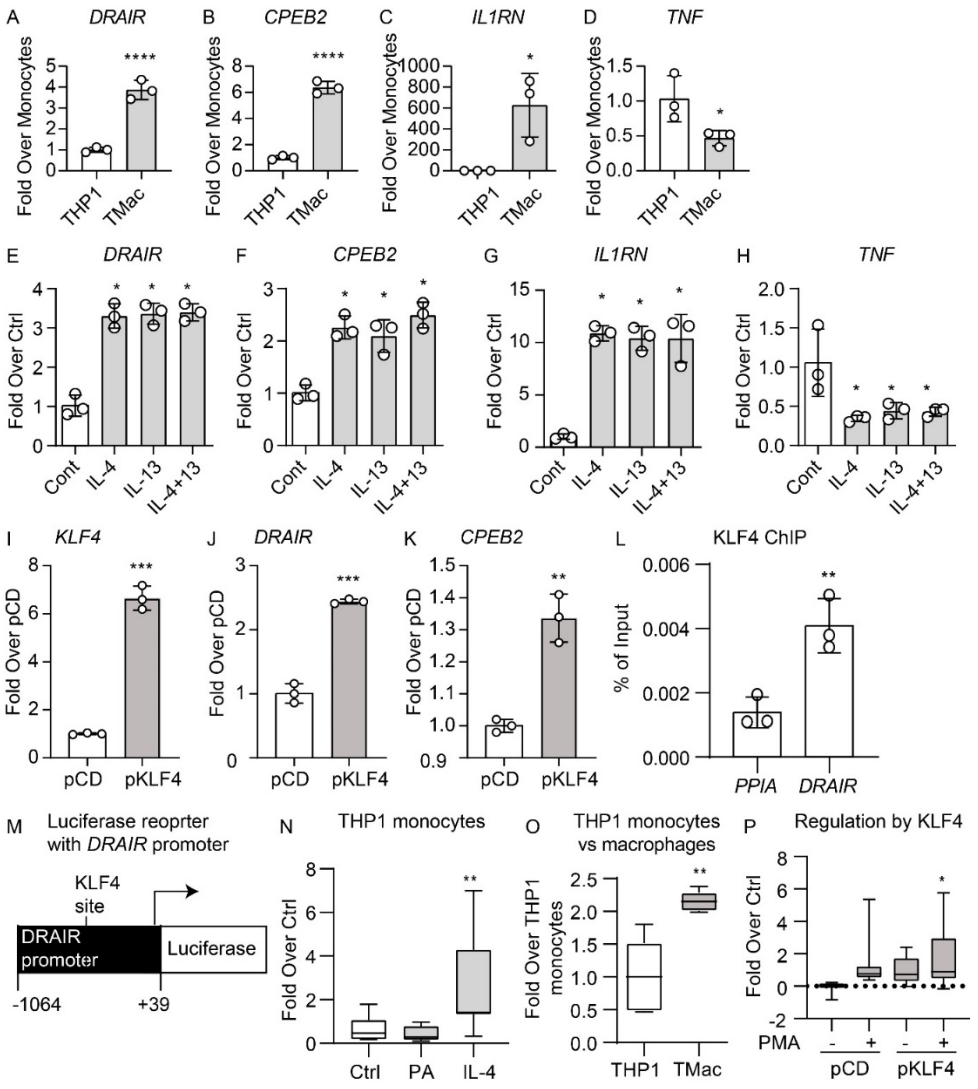

Figure 5. *DRAIR* is regulated during macrophage differentiation and by anti-inflammatory cytokines. (A-D) RT-qPCR analysis of indicated genes in THP1 monocytes (THP1) before and after differentiation into macrophages (TMac) with PMA (20 ng/ml) for 24 h. *, p<0.05 and ****, p<0.0001 as determined by unpaired t-test (n=3). (E-H) Expression of indicated genes in THP1 macrophages treated with IL-4 or IL-13 or a combination of both (20 ng/ml each). *, p<0.05, n=3. (I-K) Gene expression analysis in THP1 cells transiently transfected with control pcDNA3.1 (pCD) or KLF4 expression (pKLF4) plasmids. RT-PCRs were performed 48 h after transfection. **, p<0.01 and ***, p<0.001 versus pCD as determined by unpaired t-test, n=3. (L) QPCR analysis of ChIP

assays with KLF4 antibody with indicated promoter primers (**, p<0.01 vs PPIA promoter, n=3). (M) Schematic of the reporter plasmid (pDRluc) with DRAIR promoter cloned upstream of firefly luciferase reporter gene. KLF4 site (-760) in DRAIR promoter (not to scale). (N-P) Luciferase activities with THP1 cells co-transfected with pDRluc and internal control Renilla luciferase. In addition, plasmids pKLF4 and pCDNA3.1 were also co-transfected in panel P. One day after transfection cells were treated as indicated for 24 h. Luciferase activities are reported as fold over controls. PMA-PMA 20 ng/ml; IL-4-20 ng/ml; PA-palmitic acid (200 μM). Ctrl-control. *, p<0.05, **, p<0.01 as determined by ANOVA followed by Dunnett's multiple comparisons test (N and P, n=10-13) and unpaired t-test for (O) (n=5).

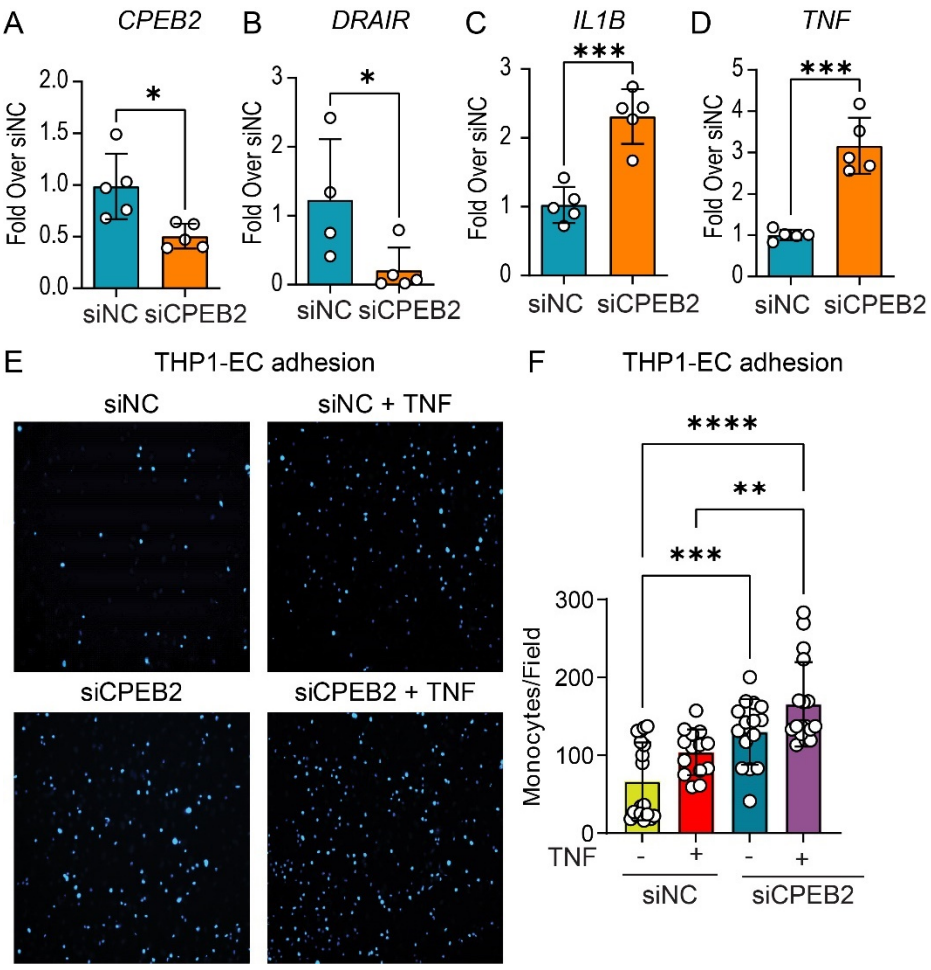

Figure 6. *CPEB2* knockdown also promotes inflammatory phenotype in THP1 monocytes.

(**A-D**) Expression of indicated genes was analyzed by RT-qPCR in THP1 cells transfected with siNC and siRNA targeting *CPEB2* (siCPEB2). *, p<0.05; ***, p<0.001, n=5, vs untreated siNC as determined by unpaired t-test. (**E-F**) Images and quantification of monocyte-endothelial cell (EC) adhesion assays. THP1 monocytes transfected with siCPEB2 or siNC were treated ± TNF-α (10 ng/ml, 3 h), fluorescently labeled with DAPI, and incubated with EC plated in 24 well plates. EC monolayers were washed with PBS and images were collected using a fluorescent microscope. Bound monocytes (blue color spots) were counted using Image J software. **, p<0.01, ***,

p<0.001, ****, p<0.0001 vs untreated siNC and versus untreated siCPEB2 as determined by ANOVA and Sidak's multiple comparisons test (n=16-19).

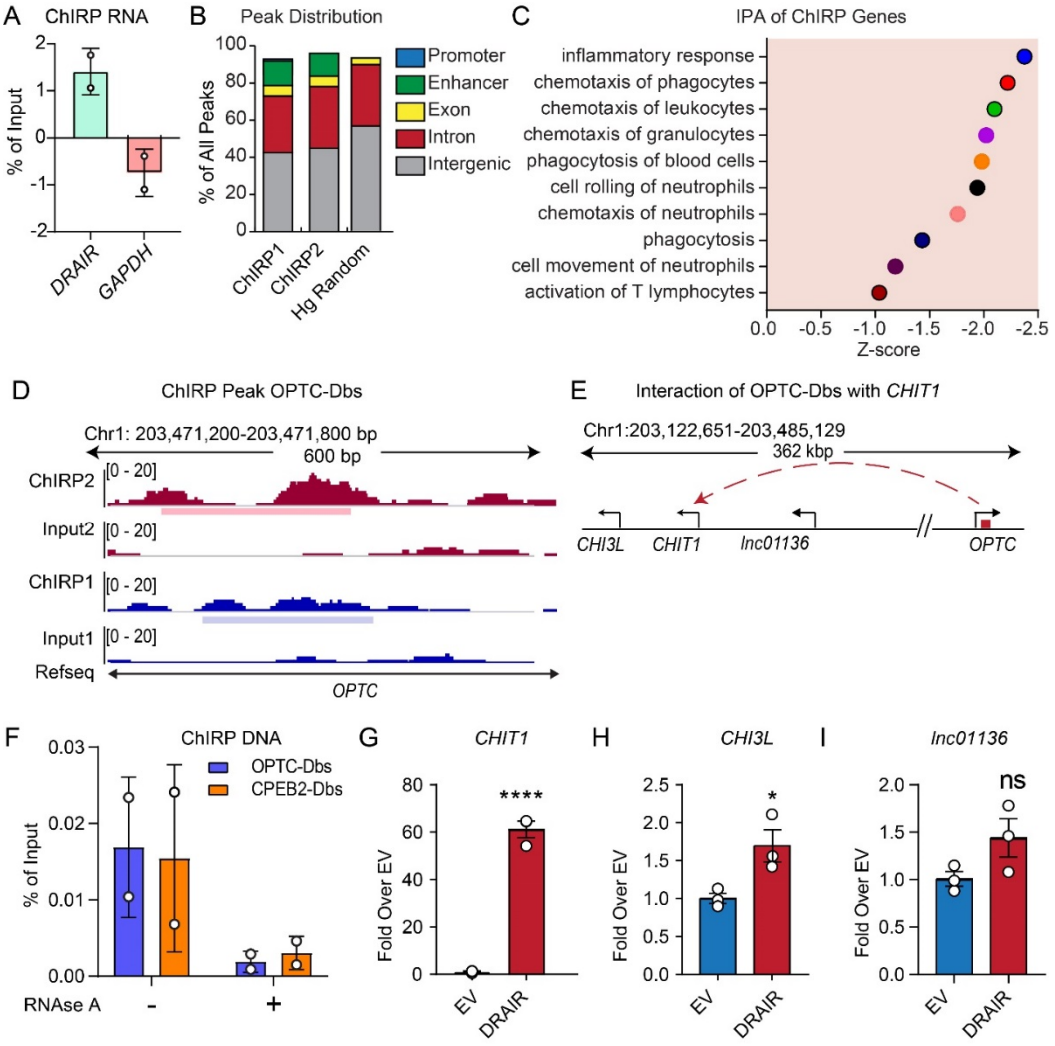

Figure 7. ChIRP analysis reveals *DRAIR* binding sites on chromatin.

(**A**) RT-qPCR analysis of RNA from ChIRP assays with indicated primers. % of input values from two experiments were log transformed. ChIRP assays were performed using biotinylated *DRAIR* antisense oligonucleotides in THP1 cells. RNA-recovered from ChIRP assays was analyzed by RT-qPCR and DNA by DNA-sequencing (ChIRP-seq). (**B**) Genomic distribution of *DRAIR* binding sites (Dbs) identified from ChIRP-seq analysis (**C**) GO terms enriched in genes nearby (± 250 kb) Dbs as determined by IPA. (**D-E**). Schematic of Dbs in the intronic region of *OPTC* gene (OPTC-Dbs) and its potential interaction with upstream region of *CHIT1* gene (**E**) identified using Hi-C plotter (CHiCP) tool. ChIRP1 and ChIRP2 in panels B and D refer to duplicates. (**F**) qPCR analysis of ChIRP-DNA using primers for indicated DRAIR binding sites.

THP1 cell lysates were treated ± pancreatic ribonuclease A (RNase A) and ChIRP assays performed with biotinylated *DRAIR* probes. RNase A treated samples served as negative controls. % of input values from two experiments were log transformed. (**G-I**) RT-qPCR analysis of indicated genes in THP1 cells over-expressing *DRAIR* (DRAIR) versus control vector (EV). *, $p<0.05$; ****, $p<0.0001$ versus EV as determined by unpaired t-test (n=3).

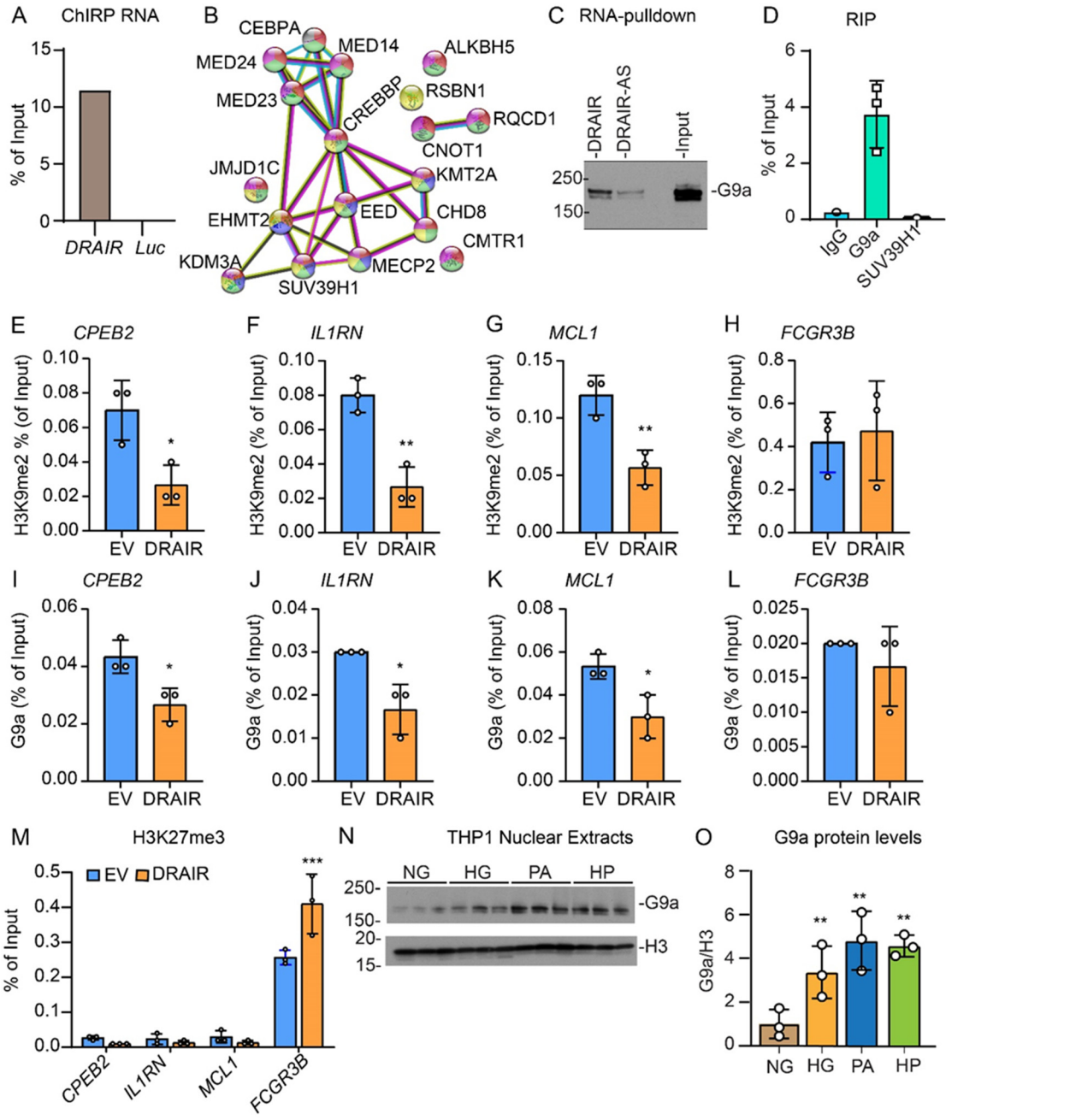

Figure 8. ***DRAIR*** **interacts with G9a and alters levels of repressive histone modifications.**

(A) RT-qPCR of RNA recovered from ChIRP with *DRAIR* probes or negative control luciferase (LUC) probes. Cell lysates from THP1 monocytes overexpressing *DRAIR* were subjected to ChIRP assays with biotinylated *DRAIR* probes and negative control biotinylated LUC probes. ChIRP complexes were captured on streptavidin beads, and RNA from an aliquot of beads was

analyzed by RT-QPCR with *DRAIR* primers. (**B**) The nucleic acid-protein complexes from ChIRP were fractionated on SDS-PAGE and subjected to Mass-spectrometry to identify proteins interacting with *DRAIR* probes. STRING analysis of indicated *DRAIR* interacting proteins identified by ChIRP-Mass spectrometry (Supplementary Figure 7). Colors represent GO Biological functions shown in Supplementary Fig. 7. (**C**) Immunoblotting of proteins from RNA-pull down assays using *DRAIR* (DRAIR) and *DRAIR* antisense (DRAIR-AS) probes with G9a antibody. (**D**) RT-qPCR analysis of RNA recovered after RNA-immunoprecipitation with indicated antibodies. (**E-M**) QPCR analysis of DNA recovered from ChIP assays using lysates from THP1 cells overexpressing *DRAIR* (DRAIR) and empty vector pcDNA3.1 (EV) with antibodies against H3K9me2 (**E-H**), G9a (**I-L**) and H3K27me3 (**M**) using indicated gene promoter primers. (**N-O**) Immunoblotting of THP1 nuclear extracts with indicated antibodies (**N**) and quantification of G9a in nuclear extracts (**O**). THP1 cells were treated with NG (5.5 mM glucose) and HG (25 mM glucose) for 72 h. Palmitic acid (PA, 200 μM) was also added in the final 24 h to NG (PA) and HG (HP) treated cells. (*, $p<0.05$; **, $p<0.01$, ***, $p<0.001$ (n=3) as determined by unpaired t-test (**E-L**) and one-way ANOVA followed by multiple testing (**M, O**).

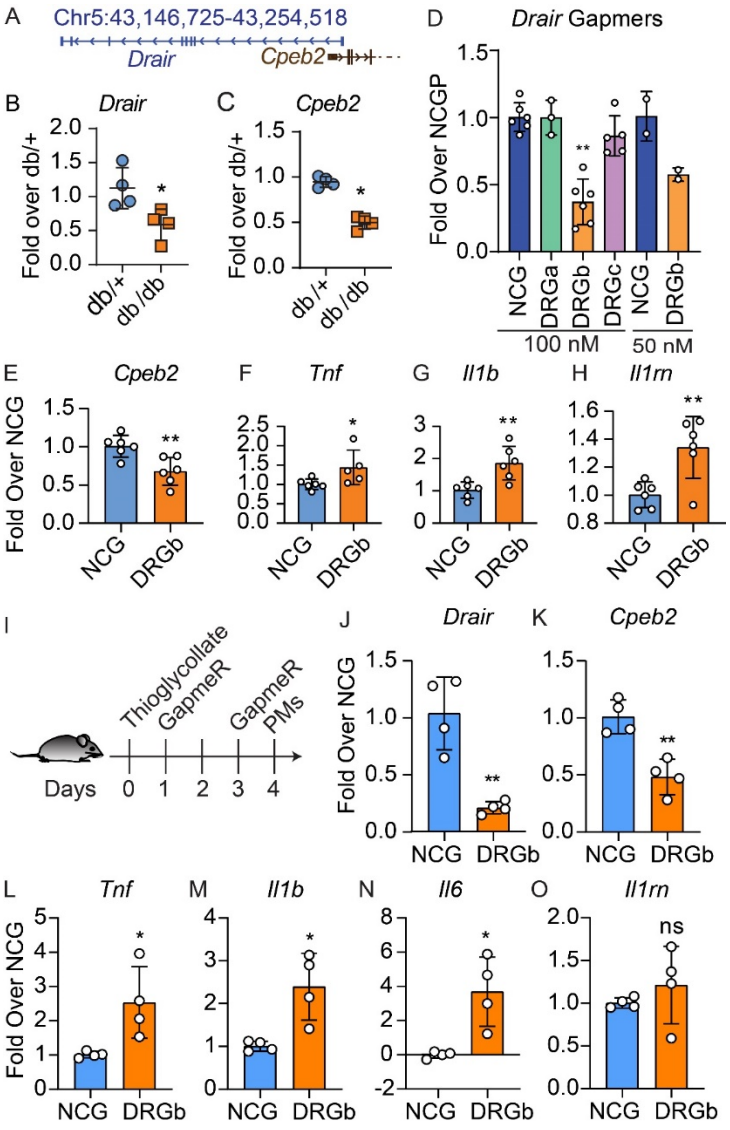

Figure 9. Mouse orthologous *Drair* is downregulated in macrophages from T2D mice and regulates inflammatory phenotype in macrophages.

(**A**) Genomic organization of *Drair* and *Cpeb2* in the mouse genome (mm9). (**B-C**) RT-qPCR analysis of *Drair* in peritoneal macrophages (PMs) from type2 diabetic db/db mice versus genetic control db/+ mice. *, p<0.05 as determined by unpaired t-test (n=4). (**D**) RT-qPCR analysis of RAW cells transfected with control (NCG) and indicated *Drair* GapmeRs (DRGa, DRGb, and DRGc) (n=2-6). (**E-H**) RT-qPCR analysis of indicated genes after *Drair* knockdown with DRGb GapmeR (DRGb) versus NCG GapmeR in RAW cells *, p<0.05, **, p<0.01 (paired t-

test). (**I**) Experimental design for *Drair* knockdown in C57BL/6 mice with GapmeRs (NCG or DRGb). (**J-O**) Gene expression analysis in PMs from C57BL/6 mice treated with NCG or *Drair* (DRGb) GapmeRs. *, $p<0.05$; **, $p<0.01$ versus NCG as determined by unpaired t-test (n=4).

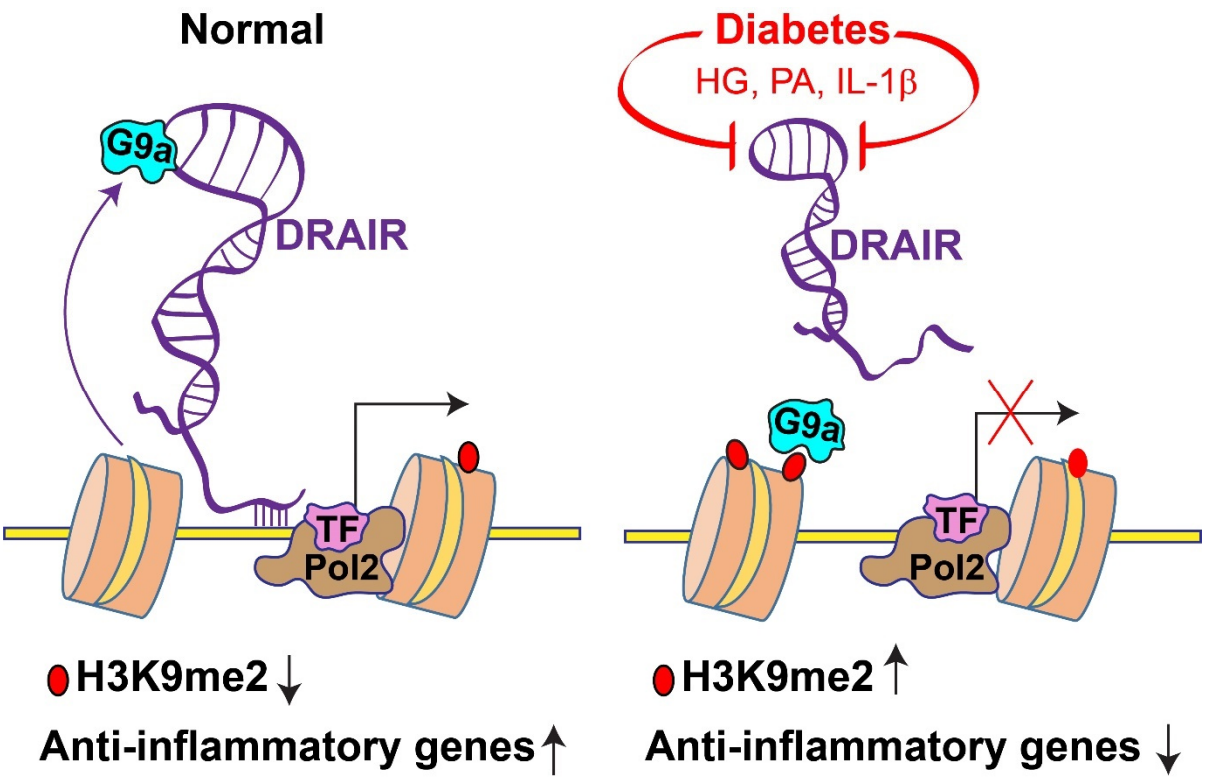

Figure 10. Schematic of DRAIR dysregulation in diabetes and epigenetic mechanisms of DRAIR actions. Under normal physiological conditions, lncRNA *DRAIR* reduces enrichment of repressive histone modifications, such as H3K9me2, at key anti-inflammatory genes, by preventing recruitment of histone methyltransferase G9a (EHMT2), which allows the normal expression of these anti-inflammatory genes. However, under diabetic conditions, downregulation of *DRAIR* and upregulation of G9a reverses these events, leading to repression of anti-inflammatory genes, activation of monocytes and chronic inflammation.